

Joana Margarida Cardoso Serra Martins

# EVALUATION OF THE POTENTIAL ANTI-INFLAMMATORY AND NEUROPROTECTIVE EFFECT OF A FAAH INHIBITOR IN GLAUCOMA MODELS

Dissertação para a obtenção do grau de Mestre em Biotecnologia Farmacêutica sob orientação científica do Doutor António Francisco Rosa Gomes Ambrósio e do Doutor Luís Fernando Morgado Pereira Almeida e apresentada à Faculdade de Farmácia da Universidade de Coimbra.

Setembro de 2015



UNIVERSIDADE DE COIMBRA



On the front page:

Retinal Ganglion Cells stained with brn3a (red) in retinal explants. Cell nuclei stained with DAPI (blue).



**Evaluation of the potential anti-inflammatory and neuroprotective effect of a FAAH inhibitor in glaucoma models**

**Avaliação do potencial efeito anti-inflamatório e neuroprotetor de um inibidor da FAAH em modelos de glaucoma**

Joana Margarida Cardoso Serra Martins

Dissertação apresentada à Faculdade de Farmácia da Universidade de Coimbra para cumprimento dos requisitos necessários à obtenção do grau de Mestre em Biotecnologia Farmacêutica. Este trabalho foi realizado no Centro de Oftalmologia e Ciências da Visão, no Instituto de Imagem Biomédica e Ciências da Vida (IBILI) da Faculdade de Medicina da Universidade de Coimbra, sob a orientação científica do Doutor António Francisco Rosa Gomes Ambrósio e do Doutor Luís Fernando Morgado Pereira Almeida

Universidade de Coimbra

2015



Execution of this work was supported by:

AIBILI, Strategic Project FCT (PEst-C/SAL/UI3282/2011/2013 and ID/NEU/04539/2013)  
and COMPETE-FEDER; Portugal





“Os dias prósperos não vêm por acaso, são granjeados, como as searas, com muita fadiga e com muitos intervalos de desalento.”  
Camilo C. Branco



## **Agradecimentos**

Na elaboração desta tese contei com o importante apoio, esforço e dedicação de várias pessoas, às quais vou agradecer e mencionar de seguida.

Primeiramente começo por agradecer ao Doutor Francisco Ambrósio, orientador desta tese, por ter permitido que conjugasse o meu trabalho no projeto em colaboração com a AIBILI, com estes 2 anos de mestrado e por me ter aceitado no seu grupo de investigação para desenvolver este trabalho científico. Obrigada pela orientação, por me ter proporcionado todas as condições para a realização desta tese e pela confiança depositada em mim. Agradeço também toda a partilha de conhecimento que contribuiu para o meu desenvolvimento pessoal e académico.

Agradeço também ao Professor Luís Almeida, também orientador desta tese, pelo apoio e disponibilidade ao longo deste ano.

Gostaria também de agradecer ao Professor Patrício Soares da Silva e ao seu laboratório na BIAL, por terem quantificado os Níveis de endocanabinoides e a atividade da FAAH nas “minhas” amostras.

Agradeço também aos meus colegas de laboratório e de trabalho, sem a vossa boa disposição, alegria e apoio teria sido muito mais difícil. Obrigada por todos os piqueniques, “happy hours” e momentos de descontração e por ao longo destes anos (sim, já lá vão 4 anos que estamos juntos!) sempre me ajudarem, me ensinarem e me apoiarem nos bons e nos maus momentos! Obrigada Tânia, Raquel Boia, Sandra, Tiago, Catarina Neves, Filipa, João, Inês, Elisa, Raquel Santiago, Maria, Catarina Gomes, Sónia, António, Paulo, Filipe, Dan, Joana Silva, Joana Duarte, Helena, Marlene, Rafael e Miguel. Agradeço também à Carla Marques pelo apoio e amabilidade. Não podia também deixar de agradecer à Susana, que nunca me deixou de mãos atadas por falta de material e por toda a amizade.

Queria agradecer em especial:

À Filipa pelo companheirismo, por todas as palavras de incentivo e pela amizade.

À Catarina Neves por todas as conversas, por todas as divertidas tardadas de explantes e pela motivação mútua!

À Tânia por todo o apoio, por me teres ajudado sempre ao longo desta tese, por me

teres orientado, por teres sido companheira e por toda a amizade!

Ao João pelo companheirismo, pela constante boa disposição e pela disponibilidade sempre demonstrada.

À minha companheira de sempre no lab e de gabinete, à Sandra, que sempre me incentivou, sempre teve uma palavra amiga e sempre me chamou a atenção para os meus erros. Obrigada pela amizade!

À Raquel Boia por todo o incentivo, por todas as chamadas de atenção, pelos momentos de descontração e pelo companheirismo. Obrigada por todas as palavras de apoio e motivação, pela disponibilidade e sobretudo pela amizade!

Agradeço também aos meus colegas de casa, da como nós chamamos “Casa do Degredos”, João, Jorge, Fred, André, Rita, Patrícia e Daniela. Obrigada por todas as conversas de incentivo, por baixarem o som da música/tv/pc quando eu precisava de me concentrar/dormir, por me fazerem rir e descontrair no dia-a-dia! Agradeço em especial à minha Pati, por sempre me ouvir a que horas fosse, por sempre me apoiar e por toda a amizade.

Gostaria também de agradecer aos meus amigos do Mestrado, os meus companheiros de grandes sagas de trabalhos, de estudo e de grandes noitadas também. Obrigada pelo apoio e pela amizade Vânia, Helena, Marcelo, Jorge, João, Nelson, Inês e Luís.

Não poderia também deixar de agradecer às minhas manas, Mary Jane e Diana. Obrigada por terem aguentado as saudades com paciência nestes últimos tempos, obrigada por estarem sempre do meu lado, por me terem dado alento e motivação nesta etapa da minha vida. Obrigada por me ouvirem sempre com muita paciência e amizade, por me fazerem sorrir sempre, por todos os nossos momentos de cumplicidade e por partilharem comigo os dias bons e os dias menos bons. *We are better when we are together!*

Quero também agradecer ao meu pessoal de CB city, por estarem sempre comigo, por terem aguentado as saudades e por apesar da distância sempre se fazerem presentes. Obrigada por todos os fins-de-semana de descontração, de sorrisos, gargalhadas e calinadas. Obrigada Rita, Paulinha, Carla, Ana Vaz, Margarida, Vânia, Sara Piki, Teresa, Marisa, Agostinho e Rita Henriques!

Agradeço também à minha família pelo constante apoio, por sempre me chamarem a atenção dos meus erros e por sempre me baterem palmas nas minhas vitórias, por estarem sempre presentes em todas as etapas da minha vida, e esta não podia faltar. Quero agradecer em especial aos meus pais e ao meu irmão, que são o meu tudo, são a minha casa e o meu porto de abrigo. Obrigada por estarem sempre de mão dada comigo, por me apoiarem sempre nas minhas decisões mais difíceis e por me terem educado para ser a pessoa que sou hoje. Obrigada por me aturarem quando estou de mau humor e por sempre me fazerem sorrir, mesmo quando tenho obstáculos para ultrapassar.

Por último, quero agradecer aos meus avós que embora já não estejam aqui presencialmente, estão sempre comigo. Em especial agradeço às minhas avós, as matriarcas da família que me criaram, que me mimaram, que foram como segundas mães e que continuam a olhar por mim, estejam onde estiverem. Obrigada minhas estrelinhas no céu.



## Table of contents

<b>Abbreviations</b> .....	<b>iii</b>
<b>Resumo</b> .....	<b>vii</b>
<b>Abstract</b> .....	<b>ix</b>
<b>1. Introduction</b> .....	<b>3</b>
1.1. Anatomy of the Eye .....	3
1.2. The Retina .....	4
1.2.1. Retinal Structure .....	4
1.2.2. Retinal Neurons .....	5
1.2.3. Retinal Glial Cells .....	7
1.2.4. Blood Vessels .....	9
1.3. Glaucoma .....	10
1.3.1. Glaucoma and Neuroinflammation .....	12
1.3.2. Glaucoma and Neuroprotection .....	13
1.3.3. Animal Models of Glaucoma .....	14
1.4. Cannabis and Endocannabinoids .....	15
1.4.1. Endocannabinoid System .....	17
1.4.1.1. Endocannabinoid Receptors .....	18
1.4.2. Endocannabinoid System in the Eye .....	19
2. Aims .....	21
<b>3. Methods</b> .....	<b>25</b>
3.1.1. Animals .....	25
3.1.2. Retinal Organotypic Cultures .....	25
3.1.3. Drug Exposure to Retinal Organotypic Cultures .....	25
3.1.4. Immunohistochemistry .....	26
3.1.5. TUNEL Assay .....	27
3.1.6. Image Analysis .....	28

## Table of contents

3.1.7.	Endocannabinoid Levels in Retinal Explants.....	28
3.1.8.	Evaluation of FAAH Activity in Retinal Explants.....	29
3.1.9.	Animal Training and Handling.....	30
3.1.10.	IOP Measurements.....	30
3.1.11.	Animal Model of Ocular Hypertension.....	31
3.1.12.	Drug Preparation and administration to animals with or without ocular hypertension.....	32
3.1.13.	Statistical Analysis.....	32
<b>4.</b>	<b>Results</b> .....	<b>37</b>
4.1.	Effect of EVC on IOP.....	37
4.2.	Effect of URB597 and O-2050 administration in IOP in animals with and without ocular hypertension.....	38
4.3.	URB597 inhibits FAAH activity in retinal explants.....	41
4.4.	URB597 increases endocannabinoids levels in retinal explants.....	41
4.5.	Evaluation of the effect of FAAH inhibitor on apoptotic cell death in retinal explants.....	43
4.6.	Effect of elevated hydrostatic pressure (EHP) in RGC survival.....	44
4.7.	Evaluation of the potential effect of FAAH inhibitor, URB597, in microglial morphology in retinal explants.....	45
4.8.	Evaluation of the potential effect of FAAH inhibitor, URB597, in microglial iNOS immunoreactivity in retinal explants.....	47
<b>5.</b>	<b>Discussion</b> .....	<b>53</b>
<b>6.</b>	<b>Conclusions</b> .....	<b>61</b>
<b>7.</b>	<b>Future perspectives</b> .....	<b>61</b>
<b>8.</b>	<b>References</b> .....	<b>65</b>

**Abbreviations**

2-AG	2-arachidonoyl glycerol
AC	Adenylate cyclase
AEA	N-arachidonylethanolamide
ARVO	<i>Association for Research in Vision and Ophthalmology</i>
BDNF	Brain-derived neurotrophic factor
BRB	Blood-retinal barrier
BSA	Bovine serum albumin
CGR	Células ganglionares da retina
CNS	Central nervous system
CPM	Counts per minute
CVE	Cauterização veias episclerais
DIV	Days <i>in vitro</i>
DMEM/F-12	Dulbecco's modified Eagle medium: Nutrient Mixture F-12
DMSO	Dimethyl sulfoxide
EHP	Elevated hydrostatic pressure
EMT	Endocannabinoid membrane transporter
EVC	Episcleral vein cauterization
FAAH	Fatty acid amide hydrolase
FBS	Fetal bovine serum
GABA	Gamma-aminobutyric acid
GCL	Ganglion cell layer
GFAP	Glial fibrillary acidic protein
i.p.	Intraperitoneal injection
iBRB	Inner blood-retinal barrier
IL-1 $\beta$	Interleukin-1 $\beta$
IL-6	Interleukin-6
ILM	Inner limiting "membrane"
INL	Inner nuclear layer
IPL	Inner plexiform layer
iNOS	Inducible nitric oxide synthase
iNOS-IR	Inducible nitric oxide synthase immunoreactivity

## Abbreviations

IO	Inferior oblique muscle
IOP	Intraocular pressure
IR	Inferior rectus muscle
IS	Inner segments
LC-MS/MS	Liquid chromatography coupled with tandem mass spectrometry
LPS	Lipopolysaccharide
LR	Lateral rectus muscle
MAGL	Monoacylglyceride lipase
MAPK	Mitogen-activated protein kinase
MR	Medial rectus muscle
NFL	Nerve fiber layer
NGS	Normal goat serum
NO	Nitric oxide
o.n.	Overnight
oBRB	Outer blood-retinal barrier
OEA	Oleylethanolamide
OLM	Outer limiting “membrane”
ONH	Optic nerve head
ONL	Outer nuclear layer
OPL	Outer plexiform layer
OS	Outer segments
PBS	Phosphate buffer saline
PEA	Palmitoylethanolamide
PHE	Pressão hidrostática elevada
PIO	Pressão intraocular
PKA	Protein kinase A
RGC	Retinal ganglion cell
ROS	Reactive oxygen species
RPE	Retinal pigment epithelium
RT	Room temperature
SO	Superior oblique muscle
SR	Superior rectus muscle
THC	$\Delta$ 9-tetrahydrocannabinol
TM	Trabecular meshwork

TNF	Tumor necrosis factor
TUNEL	TdT-mediated dUTP nick-end labeling
virodhamine	Arachidonylethanolamine



## Resumo

O glaucoma é a segunda causa de cegueira a nível mundial e é caracterizado pela perda progressiva de células ganglionares da retina (CGR). A pressão intraocular (PIO) é considerada o maior fator de risco para desenvolver glaucoma, e a redução da PIO é atualmente a única terapia utilizada. Contudo, apesar de um controlo adequado da PIO uma percentagem significativa de doentes continua a perder visão. Várias evidências têm demonstrado que a neuroinflamação tem um papel importante na patogénese do glaucoma. Em situações de neuroinflamação, as células da microglia ficam ativadas e libertam mediadores inflamatórios, os quais podem iniciar e perpetuar processos degenerativos e a morte das CGR.

A enzima hidrolase de ácidos gordos com um grupo amida (do inglês *fatty acid amide hydrolase*, FAAH) é considerada o mediador primário da hidrólise dos endocanabinóides, tais como anandamida (AEA), oleoiletanolamina (OEA), e palmitoiletanolamina (PEA). O aumento da resposta aos endocanabinóides pode ser alcançado com a inibição da atividade da FAAH, bem como através da inibição do seu transportador. Foi descrito que o aumento local dos níveis de endocanabinóides, particularmente da AEA, pode complementar eficazmente estratégias neuroprotetoras para o tratamento de doenças degenerativas da retina, como o glaucoma. Além disso, tendo em conta as propriedades dos endocanabinóides como hipotensores oculares, e os seus efeitos neuroprotetores e anti-inflamatórios, os inibidores da FAAH têm potencial para reduzir a PIO e proteger as CGR, reforçando assim a sua relevância para o tratamento do glaucoma.

Neste estudo, pretendeu-se avaliar o potencial efeito de um inibidor da FAAH (URB597) na diminuição da PIO num modelo de hipertensão ocular (cauterização das veias episclerais – CVE). Além disso, pretendeu-se investigar, pela primeira vez, os potenciais efeitos neuroprotetores e anti-inflamatórios do URB597 num modelo de pressão hidrostática elevada (PHE), com o objetivo de mimetizar uma situação de PIO elevada, em explantes de retina de rato.

Em animais submetidos a CVE, a PIO aumentou significativamente, durante pelo menos 7 dias. A administração do URB597 diminuiu significativamente a PIO, e este efeito pareceu ter sido mediado pela ativação dos recetores dos endocanabinóides do tipo CB<sub>1</sub>. A atividade da FAAH foi fortemente inibida pelo URB597 em culturas organotípicas de retina. Além disso, o composto URB597 aumentou os níveis de AEA,

OEA e PEA nestas culturas. A exposição de explantes de retina a PHE reduziu significativamente a sobrevivência das CGR. O tratamento com URB597 inibiu a diminuição do número de CGR. Contudo o efeito protetor do URB597 pareceu não ter sido mediado pela ativação dos recetores CB<sub>1</sub>. Além disso, o composto URB597 inibiu o aumento da imunoreatividade da isoforma indutível da sintase do monóxido de azoto (do inglês *inducible nitric oxide synthase*, iNOS) em células da microglia, induzida pela PHE em explantes de retina. No entanto, uma vez mais, o efeito inibitório do URB597 não pareceu ter sido mediado pelo recetor CB<sub>1</sub>.

Em conclusão, os resultados apresentados nesta tese indicam claramente que a enzima FAAH representa um potencial alvo terapêutico num contexto de glaucoma, que vale a pena investigar, uma vez que a inibição da FAAH tem potencial para diminuir a PIO, para controlar a neuroinflamação e para proporcionar neuroprotecção contra a degenerescência das CGR.

**Palavras-chave:** Glaucoma, pressão intraocular, endocannabinóides, inibidor da FAAH, neuroprotecção da retina, neuroinflamação, cauterização das veias episclerais, pressão hidrostática elevada, recetor CB<sub>1</sub>.

## Abstract

Glaucoma is the second leading cause of blindness in the world and is characterized by progressive loss of retinal ganglion cells (RGCs). Elevated intraocular pressure (IOP) is considered the primary risk factor for the development of glaucoma and lowering IOP is the only clinical therapy available. However, some patients continue to lose vision despite successful IOP control. It has been shown that neuroinflammation plays an important role in the pathogenesis of glaucoma. During neuroinflammatory events, microglial cells become activated and release pro-inflammatory mediators, which in turn can initiate and perpetuate degenerative processes and RGC death.

The enzyme fatty acid amide hydrolase (FAAH) is thought to be the primary mediator of the hydrolysis of released endocannabinoids, such as anandamide (AEA), oleoyletanolamine (OEA), and palmitoyletanolamine (PEA). Enhancement of endocannabinoid responses can be achieved with inhibition of FAAH activity, as well as through inhibition of its endocannabinoid transporter. It was described that increasing local endocannabinoid levels, particularly AEA, may be an effective supplement to the arsenal of neuroprotective strategies for retinal degenerative diseases, such as glaucoma. Moreover, taking into account the ocular hypotensive properties of endocannabinoids, in addition to its neuroprotective and anti-inflammatory effects, FAAH inhibitors have the potential to decrease IOP, thereby strengthening its relevance to treat glaucoma, protecting RGCs against degeneration.

In this study, we aimed to assess the potential effect of a FAAH inhibitor (URB597) in decreasing IOP in a model of ocular hypertension (episcleral vein cauterization - EVC). In addition, another goal was to investigate, for the first time, the potential neuroprotective and anti-inflammatory effects of URB597 in a model of elevated hydrostatic pressure (EHP), mimicking elevated IOP, in rat retinal explants.

In animals submitted to EVC, the IOP was significantly increased, at least for 7 days. The administration of URB597 significantly decreased IOP, and this effect seemed to be partially mediated by CB<sub>1</sub> receptor activation. The activity of FAAH was strongly inhibited by URB597 in retinal organotypic cultures. Moreover, URB597 increased the levels of AEA, OEA, and PEA in these cultures. Exposure of retinal explants to EHP significantly reduced RGC survival. Treatment with URB597 inhibited the decrease in the number of RGCs, but this protective effect did not seem to be mediated by the activation of CB<sub>1</sub> receptors. In addition, URB597 inhibited the increase of iNOS immunoreactivity in microglial cells induced by EHP exposure in

## Abstract

retinal explants, but the CB<sub>1</sub> receptor did not seem to mediate this inhibitory effect of URB597.

In summary, our results clearly show that FAAH enzyme represents a potential therapeutic target worth to investigate in the context of glaucoma, once FAAH inhibition has the potential to decrease IOP, control neuroinflammation, and provide neuroprotection against RGC degeneration.

**Keywords:** Glaucoma, intraocular pressure, endocannabinoids, FAAH inhibitor, retinal neuroprotection, neuroinflammation, episcleral vein cauterization, elevated hydrostatic pressure, CB<sub>1</sub> receptor.

# CHAPTER I

---

*Introduction*



## I. Introduction

### I.1. Anatomy of the Eye

The eye is an important organ that allows gathering information about the surrounding world. This organ is a highly specialized and organized structure that receives the light and transduces this information into electrical signals, which are processed and converted into visual images in the brain (Purves, 2004).

The outermost layer of the eye is composed by the sclera and cornea (Fig. 1). The sclera is a white fibrous and opaque tissue that helps to confer shape and protection to the internal structures of the eye. At the front of the eye, this opaque layer becomes the cornea, a transparent avascular tissue that allows the input of light into the eye causing reflection or refraction of the light that enters (Kolb, 1995;Purves, 2004).

Inner to the sclera and cornea is the uveal tract, formed by three distinct structures, the choroid, ciliary body and iris. Choroid is rich in blood vessels and its main function is the nourishment of the outer layers of the retina. The iris is the most anterior component of the uveal tract, the coloured portion of the eye that can be seen through the cornea. It contains two sets of muscles that control the size of the pupil so that more or less light is allowed to enter the eye. The ciliary body has a muscular component attached to the lens by zonule fibres, which enables the lens to change shape during accommodation, and a vascular component which produces the aqueous humour that fills the anterior and posterior chambers of the eye. Aqueous humour is produced by the ciliary processes in the posterior chamber (between the iris and the lens) and flows into the anterior chamber (between the cornea and the iris) through the pupil. The rates of aqueous humour production and drainage must be balanced to ensure a constant intraocular pressure (IOP). The drainage of the aqueous humour is processed generally through the trabecular meshwork (Schelmm's channel) (Kolb, 1995;Purves, 2004).

The innermost layer of the eye is formed by the retina, a light sensitive tissue that has the function of photoreception and transmits impulses to the brain. In addition to anterior and posterior chambers, there is a third chamber inside the eye, the vitreous chamber, located between the lens and the retina. This chamber is filled with a gelatinous substance mainly composed by collagen fibres. The vitreous humour is responsible for maintaining the eye integrity (Kolb, 1995;Purves, 2004).

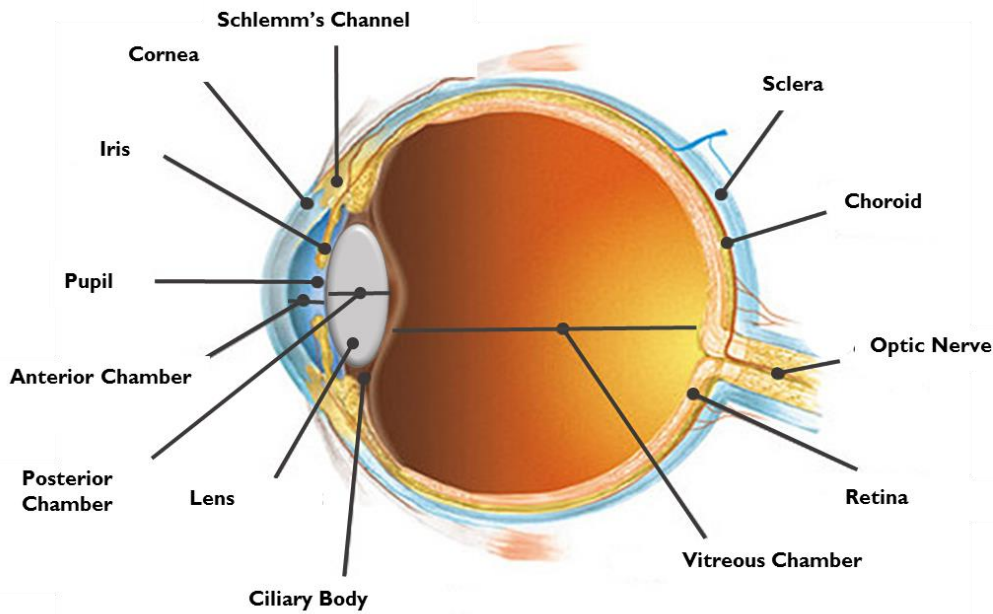


**Figure 1** - Anatomy of the human eyeball (adapted from: <http://en.excimerclinic.ru/press/stroenieglaza>).

## 1.2. The Retina

### 1.2.1. Retinal Structure

The retina, despite its peripheral location, is part of the central nervous system (CNS) and it is organized in eight different layers (Fig. 2). The retinal pigment epithelium (RPE) is the outermost one and its main role is renewing photoreceptor photopigments and phagocytosing the photoreceptor disks, being this interaction essential for visual function. Inner to RPE is the layer composed by photoreceptor outer segments (OS) which contains the visual photopigments. The cell bodies of the photoreceptors (cones and rods) are in the inner segments (IS), and form the outer nuclear layer (ONL), while the synapses between photoreceptors, bipolar, and horizontal cells occurs in the outer plexiform layer (OPL). The inner nuclear layer (INL) is composed by the cell bodies of bipolar, amacrine, and horizontal cells. The synapses between bipolar, amacrine, and retinal ganglion cells (RGCs) take place in the inner plexiform layer (IPL). The cell bodies of RGCs and some displaced amacrine cells form the ganglion cell layer (GCL). The RGC axons are responsible for carrying the visual information to the brain, and constitute the nerve fiber layer (NFL) (Kolb, 1995; Purves, 2004).

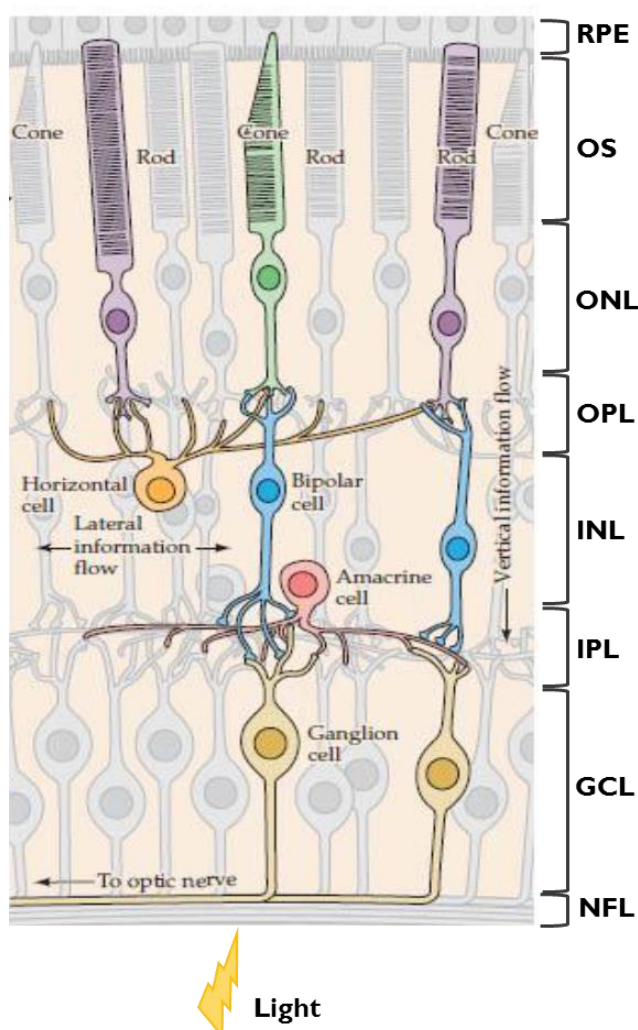


**Figure 2- Anatomy of the retina showing all the neuronal cell types.** RPE - retinal pigment epithelium; OS - photoreceptor outer segments; ONL - outer nuclear layer; OPL - outer plexiform layer; INL - inner nuclear layer; IPL - inner plexiform layer; GCL - ganglion cell layer; NFL- nerve fiber layer (adapted from (Purves, 2004)).

### 1.2.2. Retinal Neurons

The neuronal component of the retina is composed by five different types of neuronal cells: photoreceptors, bipolar cells, horizontal cells, amacrine cells, and RGCs (Fig.2).

In the vertebrate retina there are two types of photoreceptors: rods and cones. Both types have an outer segment composed of membranous disks containing light-sensitive photopigment that lies adjacent to the RPE, and an IS that contains the cell nucleus and gives rise to synaptic terminals contacting bipolar and horizontal cells (Purves, 2004). Two or three types of cone photoreceptor and a single type of rod photoreceptor are present in the mammalian retina, and its distribution in the retina is very important for visual processing. Rods contain the visual photopigment

## Introduction

rhodopsin, allowing for high light sensitivity, essential for vision under dark-dim conditions at night. In contrast, cones contain cone opsins as their visual photopigments. The cone opsins are responsible for bright light and coloured vision (Kolb, 1995). Absorption of light by the photopigments initiates a cascade of events, which lead to hyperpolarization of photoreceptor membrane, and consequently the decrease of neurotransmitter (glutamate) released by the photoreceptor synapses onto the cells they contact (Purves, 2004).

Bipolar cells are the interlocutors between the light transduction of photoreceptors and amacrine cells and RGCs. In human retina there are eleven different bipolar cell types, ten of which contact cones and one type contacts rods (Kolb, 1995). These cells, based on how they react to glutamate released from photoreceptors, can be classified into ON- and OFF-type bipolar cells, distinguishable by the type of glutamate receptor they express. The OFF-type bipolar cells express ionotropic glutamate receptors and are hyperpolarized by light. ON-type bipolar cells express metabotropic glutamate receptors and are depolarized by light (Kolb, 1995;Purves, 2004).

The RGCs are the final output neurons of the retina, collecting visual signals from bipolar and amacrine cells. RGCs can also be divided into ON- and OFF-centre, according to the bipolar cell types they contact within their receptive field. The number of ON- and OFF-centre RGC types in the retina is approximately the same, and usually the receptive field of neighbour cells overlap. This distribution allows the same retinal point to be analysed by several ON- and OFF-RGCs (Purves, 2004). These two types of RGCs are distinguished by their firing rate when they are stimulated by a small spot of light in the centre of their receptive field. When the centre of an OFF-centre RGC is exposed to light it hyperpolarizes, decreasing their discharge rate. Conversely, they depolarize when the surround receptive field is exposed to light, increasing their firing rate. ON-centre RGCs have the opposite response. They become activated when the centre is exposed to light and inactive when the surround is stimulated. Thus, OFF-centre RGCs increase their discharge rate to luminance decrements in the receptive field, whereas ON-centre RGCs increase their discharge rate to luminance increments in the receptive field (Kolb, 1995;Purves, 2004).

Horizontal cells are interneurons in the retina and modulate signal transmission between photoreceptors and bipolar cells (Kaneda, 2013). Horizontal cells' processes allow lateral interactions between photoreceptors and bipolar cells, which maintain the visual system's sensitivity to luminance contrast over a wide range of light intensities (Kolb, 1995; Purves, 2004).

Amacrine cells are interneurons, present in the INL and GCL that modulate the signal transmission between bipolar cells and RGCs. There are more than 20 classified subtypes of amacrine cells, and according to the subtype, they have different contributions for the processing of visual elements, such as contrast, colour, brightness, and movement (Purves, 2004; Kaneda, 2013).

### **1.2.3. Retinal Glial Cells**

Similarly to other CNS regions, the retina is also composed by glial cells. There are three types of glial cells in the retina: Müller cells, astrocytes and microglia, which are responsible for neuro-supporting and immunocompetent defence (Langmann, 2007).

Müller cells are the main glial cell type of the retina, spanning from the vitreal surface to subretinal space and covering all retinal layers. Müller cells are major supporting cells in regulating physiological and pathological responses of neurons and retinal vasculature. These cells have an important role in metabolism and protection providing trophic factors, removing metabolic wastes, controlling ion and water homeostasis and extracellular space volumes, participating in visual cycles, releasing neurotransmitters, regulating blood-retinal barrier (BRB) function, and modulating innate immunity (Reichenbach and Bringmann, 2013).

Astrocytes are the major glial cell type found at the optic nerve head (ONH) and at NFL, and undertake some essential functions related to the CNS homeostasis. In response to injuries, astrocytes proliferate, change their morphology, and increase glial fibrillary acidic protein (GFAP) expression; this process is designated astrogliosis (Kolb, 1995; Chong and Martin, 2015). Astrocytes are also part of the BRB, having a close association with retinal vessels and regulating its properties. Moreover, astrocytes contribute to neuronal nutrition, providing glucose, and also contribute to the regulation of extracellular potassium levels and metabolism of neurotransmitters such as GABA (Kolb, 1995).

Microglial cells are the resident macrophages in the CNS and they have an important role in the surveillance of the microenvironment. In healthy conditions, microglial cells acquire a characteristic ramified morphology extending long thin processes; this stage has been named “resting” state (Kettenmann *et al.*, 2011). In response to various stimuli associated with aging, neurodegeneration, or injury, microglia turn into the activated state, an effector phenotype, in which they migrate to the site of injury, proliferate, and phagocytose cells and cellular compartments (Bosco *et al.*, 2011; Kettenmann *et al.*, 2011). Upon activation, microglial cells release cytokines, chemokines, nitric oxide (NO), and reactive oxygen species (ROS), which could be detrimental or beneficial to the neighbouring cells (Harry, 2013). Thus, microglial cells are indispensable in the adult CNS as stabilizers and modulators of tissue homeostasis under physiological or pathological conditions (Kierdorf and Prinz, 2013).

In the retina, microglial cells are mainly located in the inner vascularized regions, *i.e.* the NFL, GCL, OPL and IPL, while they are not frequent in the INL and absent in the ONL (Santiago *et al.*, 2014). In a healthy retina, microglial cells also play important roles in tissue surveillance and intercellular communication by continuous and dynamic behavior (Lee *et al.*, 2008). In the resting state, microglial cells mainly populate the plexiform layers, and actively survey their microenvironment with extremely motile processes and protrusions (Fig. 3A) (Li *et al.*, 2015). In this state microglial cells also phagocytose the cellular debris from neurons in the INL and GCL (Langmann, 2007). In retinal insult situation, such as optic nerve damage, inflammation, light injury, intoxication, hereditary diseases or metabolic disturbance, microglia are activated immediately changing their morphology (Fig. 3B) (Saijo and Glass, 2011). Therefore, in the effector phase (Fig. 3C), microglia and/or recruited blood-derived precursors migrate to the nuclear layers and the subretinal space, where they engulf dying cell corpses (Karlstetter *et al.*, 2010).

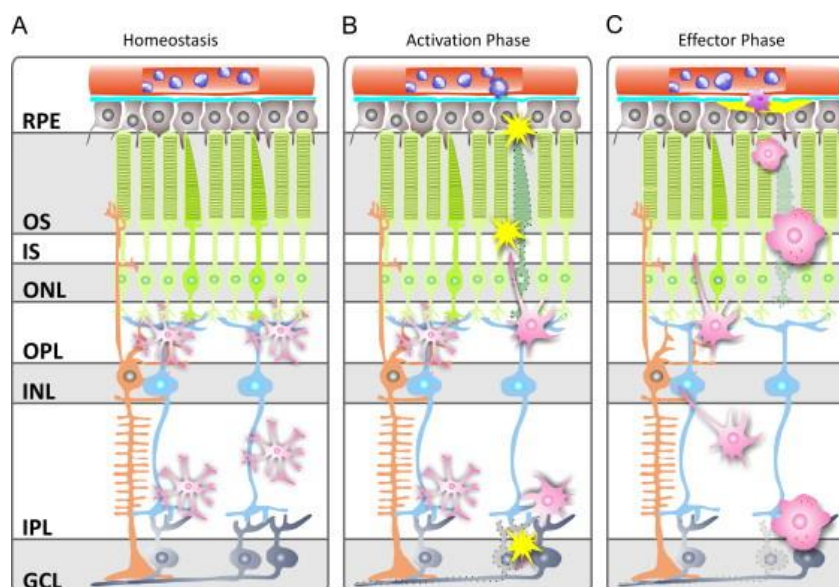


**Figure 3 - Schematic representation of three common phases of microglial activity in the retina.** (A) In the normal retina, resident microglia mainly populate the plexiform layers. With their long protrusions they continuously scan their environment, phagocytose cell debris and secrete a variety of supporting factors including neurotrophins. (B) Various different insults leading to abnormal cell functions or degeneration in the RPE, the photoreceptor layer, and the GCL rapidly alert microglia. (C) Resident microglia and/or recruited blood-derived precursors migrate to the lesion sites, where they transform into amoeboid full-blown phagocytes. These effector cells may be protective or detrimental depending on their immunological phenotype and the local cytokine milieu. RPE - retinal pigment epithelium, ONL - outer nuclear layer, OPL - outer plexiform layer, INL - inner nuclear layer, IPL - inner plexiform layer, GCL - ganglion cell layer (adapted from (Karlstetter *et al.*, 2010)).

#### 1.2.4. Blood Vessels

The retina has the higher oxygen consumption per weight of human tissue. Therefore, it needs a complex vascular system to provide oxygen and nutrients to the highly metabolically active neural retina. To accomplish this metabolic requisite, the retina is supplied by two different sources of blood vessels, the central retinal artery and the choroidal blood vessels. The central retinal artery gives rise to capillaries that innervate the inner retina, while the choroidal blood vessels supply photoreceptors in the outer retina (Klaassen *et al.*, 2013).

In order to protect the retina from potentially harmful molecules in the circulation, the BRB is divided into inner BRB (iBRB) and outer BRB (oBRB) (Fig. 4). The iBRB is formed by the tight junctions of retinal capillary endothelial cells, which are surrounded by pericytes, astrocytes, Müller cells, microglia and neurons. The oBRB consists of the tight junctions of RPE cells, and is responsible for the maintenance of the homeostasis of the outer retina. The iBRB and oBRB tight junction

proteins consist mainly of occludin, claudins, zonula occludens proteins, and junctional adhesion molecules (Cunha-Vaz *et al.*, 2011; Zhang *et al.*, 2014).

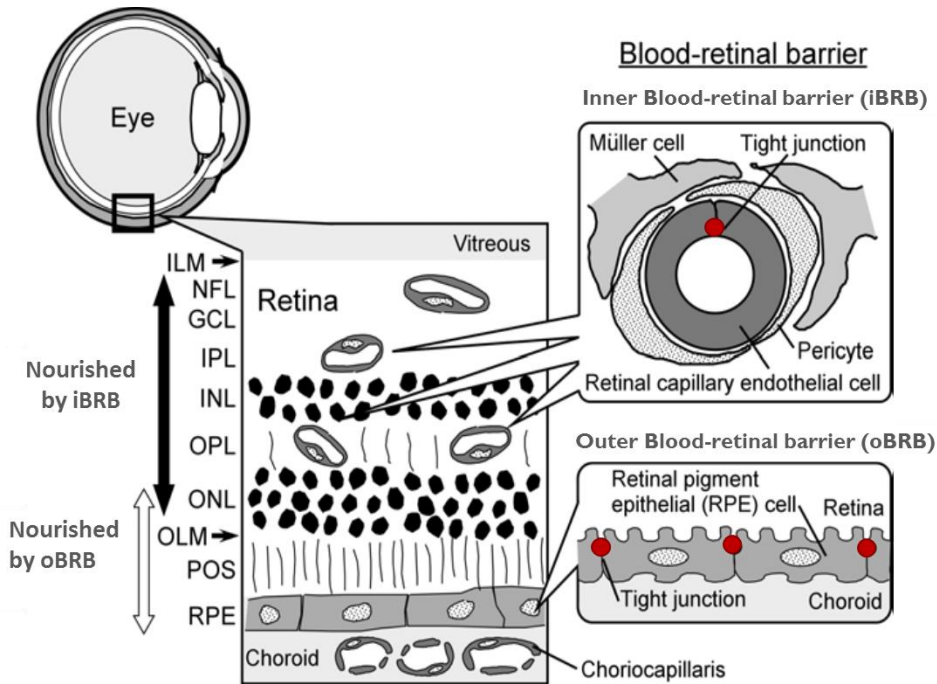


**Figure 4 - Scheme of the BRB.** The retinal cell layers are presented, as follows: RPE - retinal pigment epithelium; OS - photoreceptor outer segments; OLM - outer limiting “membrane”; ONL - outer nuclear layer; OPL - outer plexiform layer; INL - inner nuclear layer; IPL - inner plexiform layer; GCL - ganglion cell layer; NFL - nerve fiber layer; ILM - inner limiting “membrane” (adapted from (Hosoya, 2008)).

### 1.3. Glaucoma

Glaucoma refers to several optic neuropathies associated with degeneration of RGCs and their respective axons, leading to slow progressive visual field loss (Fig 5). Glaucoma is considered the second leading cause of blindness throughout the world. In 2010, at least 60.5 million people suffered from glaucoma worldwide and it is expected to increase up to 80 million by 2020 (Van de Velde *et al.*, 2015).

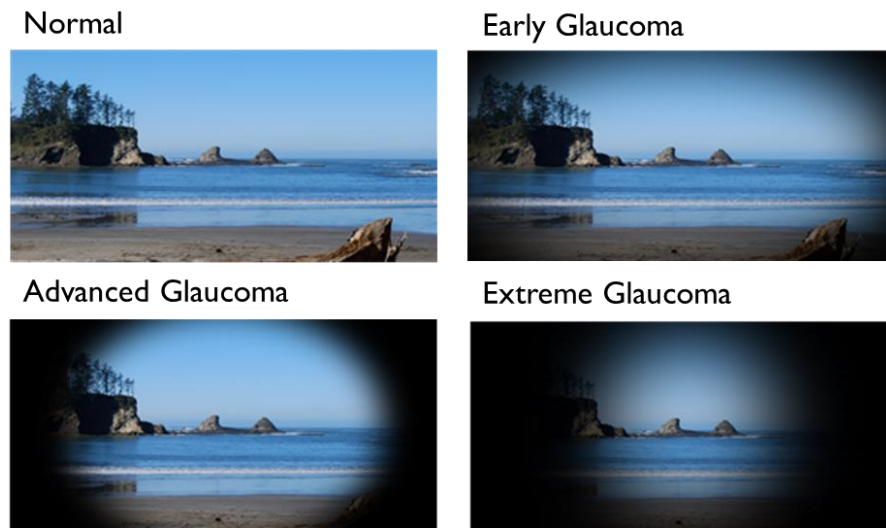


**Figure 5 – Images representative of how glaucoma affects vision at the peripheral fields, in patients at different stages of the disease** (adapted from [http://seaviewoptometry.com/eye\\_care/glaucoma-prevention.html](http://seaviewoptometry.com/eye_care/glaucoma-prevention.html)).

The pathology of glaucoma is not entirely elucidated, although it is known that there are multiple risk factors such as genetic mutations, ethnicity, age, and increased IOP. A basal IOP is needed to maintain the shape and homeostasis of the eye, and is regulated by aqueous humour production in the ciliary bodies (To *et al.*, 2002) and drainage through two mechanisms: conventional outflow, which is through trabecular meshwork and Schlemm's canal, and uveoscleral outflow (Fig. 6) (Doucette *et al.*, 2015).

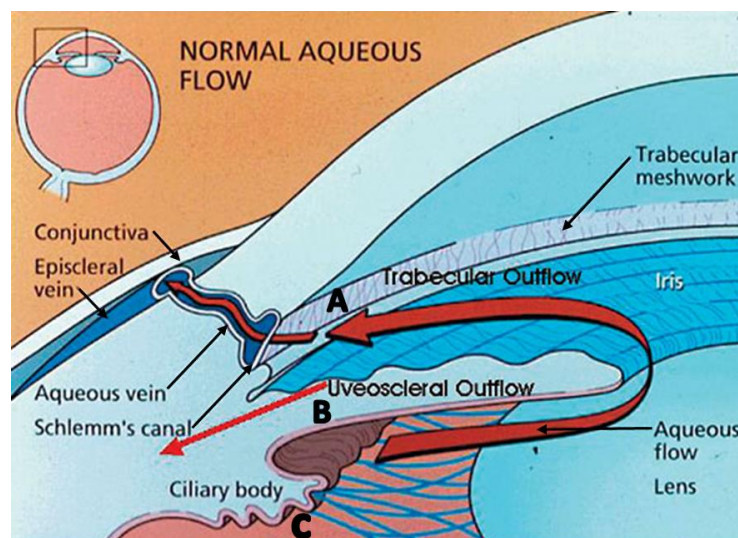


**Figure 6 - Scheme of the normal outflow of the aqueous humour.** Outflow of the aqueous humour occurs by two ways: trabecular outflow (A) and uveoscleral outflow (B). The aqueous humour formation occurs in the ciliary bodies (C) (adapted from [http://www2.cfpc.ca/cfp/2005/Sep/vol51-sep-cme-3\\_fr.asp](http://www2.cfpc.ca/cfp/2005/Sep/vol51-sep-cme-3_fr.asp)).

Glaucoma is also associated with a typical appearance of structural damage at the optic nerve head (ONH), seen as excavation of ONH, and sectoral retinal nerve fiber layer defects (Chang and Goldberg, 2012) (Fig. 7).

Since increased IOP is the major risk factor to develop glaucoma, the treatment of this disease is mainly directed towards lowering IOP, although many patients present signs of progression of this neuropathology despite well-controlled IOP (Van de Velde *et al.*, 2015). In fact, RGC degeneration can be caused by other factors such as activation of the glial cells in response to glaucomatous stress, which exhibit important links of this pathology to different components of the immune system (Tezel, 2011).

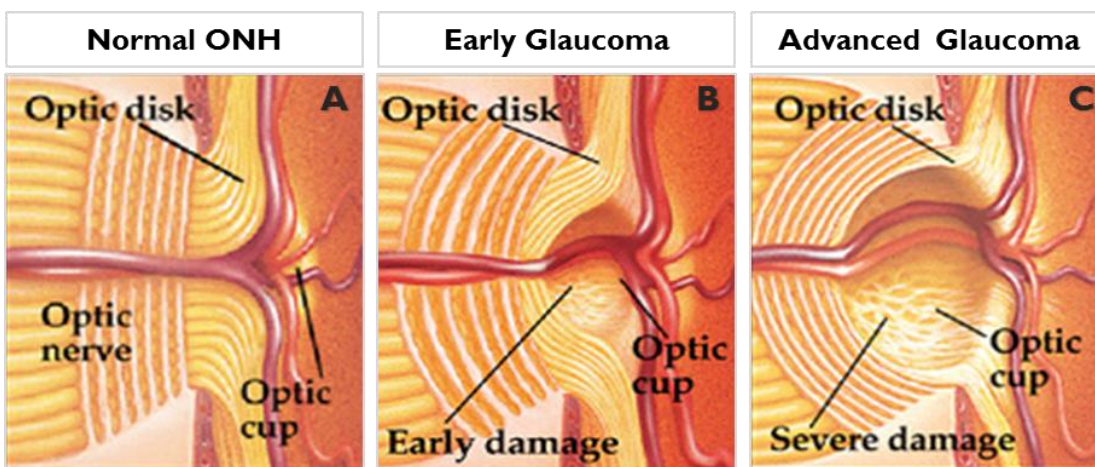


**Figure 7 - Scheme of the excavation of ONH during the progression of glaucoma. (A)** Normal ONH; **(B)** ONH in an early stage of glaucoma; **(C)** ONH in an advanced stage of glaucoma (adapted from <http://www.dreyeins.com/tests-for-glaucoma.php>).

### 1.3.1. Glaucoma and Neuroinflammation

In the pathogenesis of glaucoma, neuroinflammation has been described as an important player in disease progression, by activating glial cells that initiate an inflammatory response (Madeira *et al.*, 2015a).

Glial cells have a high level of plasticity which allows them to rapidly respond to any homeostatic imbalance by exhibiting the active phenotype with altered cell morphology and expression of cell markers (Tezel, 2011). Namely, microglial cells in glaucomatous conditions have shown alterations in morphology, gene expression, cell proliferation, cell adhesion, and immune response, compatible with a reactive phenotype. (Karlstetter *et al.*, 2010; Madeira *et al.*, 2015a). When microglial reactivity becomes excessive or prolonged, it may lead to chronic inflammation, by an excessive production of pro-inflammatory and neurotoxic factors such as tumor necrosis factor

(TNF), interleukin-6 (IL-6), interleukin-1 $\beta$  (IL-1  $\beta$ ), NO, endothelin, complement proteins and superoxide, with severe pathological effects potentially resulting in RGC loss (Karlstetter *et al.*, 2010;Almasieh *et al.*, 2012).

In several animal models of glaucoma, it has been described that microglia, Müller cells and ONH astrocytes play critical roles in glaucomatous neurodegeneration (Chong and Martin, 2015). In DBA/2J mice, which are transgenic mice with age-related ocular hypertension, microglial activation has been correlated with the loss of RGCs; reducing microglial activation has been suggested to increase RGC viability (Fernandes *et al.*, 2015).

In previous studies in our group, using retinal organotypic cultures, challenged with either elevated hydrostatic pressure (EHP) or lipopolysaccharide (LPS), microglial cells are activated and this is paralleled by an increase in the expression and release of the pro-inflammatory cytokines IL-1 $\beta$  and TNF. Moreover, adding anti-IL-1 $\beta$  and anti-TNF antibodies to the culture medium prevents RGC death triggered by EHP or LPS, indicating that RGC death is caused by microglia reactivity and particularly by pro-inflammatory cytokines (Madeira *et al.*, 2015b).

Moreover, the cross-talk between microglia and RGCs, as well as other types of retinal glia may plays an important role determining the glial behavior in a disease context, as glaucoma. Thus, targeting certain aspects of glial signalling in the retina could be a therapeutic strategy with great potential for future clinical applications (Chong and Martin, 2015).

### **1.3.2. Glaucoma and Neuroprotection**

Glaucoma is a multifactorial degenerative disease, with complex genetic and environmental factors involved in its pathogenesis (Baltmr *et al.*, 2010). As previously mentioned, RGC death is a hallmark of glaucoma, in which several mechanisms might be involved. IOP is considered the main direct inducer of RGC stress and apoptosis, although damage to RGCs may occur in the presence of normal IOP.

Several other pathogenic processes have been identified such as retinal ischemia, glial cell activation, mitochondrial dysfunction, protein misfolding, neurotrophin deprivation, oxidative stress, excitotoxicity due to raised extracellular levels of glutamate, and all may induce apoptotic RGC death in glaucoma (Baltmr *et al.*, 2010;Qu *et al.*, 2010;Chen *et al.*, 2015). Therefore, all these processes may be targeted in order to afford neuroprotection and prevent RGC loss independent of IOP elevation (Chen *et al.*, 2015).

### 1.3.3. Animal Models of Glaucoma

There are several animal models of glaucoma, including genetic models (e.g. DBA/2J mice) and inducible models of IOP elevation such as: microbead injections in the anterior chamber (Sappington *et al.*, 2010; Morgan and Tribble, 2015), glucocorticoid-induced IOP elevation (Overby and Clark, 2015), episcleral vein cauterization (EVC) (Shareef *et al.*, 1995; Urcola *et al.*, 2006), and saline injection in the episcleral veins (Morrison *et al.*, 1997).

In the microbeads model described by Sappington (2010), the IOP increases around 30% in rodents, comparing with the control eyes, and this increase is consistent during 4–5 weeks (Sappington *et al.*, 2010). In this model, there is approximately a 20% loss of ganglion cell axons in rats and mice. In the saline injection in the episcleral veins model, described by Morrison (1997), IOP is elevated from 7 to 28 mm Hg, leading to axonal damage, sclerosis of the trabecular meshwork (TM) and optic nerve damage, which is characteristic of glaucoma (Morrison *et al.*, 1997). In the glucocorticoid-induced ocular hypertension model, IOP increases in rats during 2 to 4 weeks, after the eye topical administration of dexametasone, which is a glucocorticoid, every day until 4 weeks. In this model occurs an increase in TM thickness and a decrease in TM cell number, occurring also a decrease in the thickness and in the cell number in the RGC layer (Overby and Clark, 2015). Overall, the main goal of these models is to study RGC degeneration and other related complications triggered by chronic ocular hypertension. Unfortunately, all these models have some disadvantages and sometimes are difficult to reproduce and to induce a consistent and sustained IOP increase.

EVC glaucoma model consists in cauterizing the episcleral veins of the eye, and thus blocking the outflow of the aqueous humour through the Schlemm's channel and by the uveoscleral pathway (Urcola *et al.*, 2006). By this way, IOP increases and induces retinal cell death, namely RGC death. It has been described that in rats submitted to EVC model, not only occurs RGC degeneration, but also amacrine and bipolar cells damage; the loss of these cells causes changes in visual direction selectivity processing that could also be associated with glaucoma (Danas *et al.*, 2006; Hernandez *et al.*, 2009). In addition, it has been reported that RGC death, induced by EVC, activates astrocytes and Müller cells. Astroglisis also may potentially exacerbate the glaucomatous process by overexpressing toxins, producing a direct toxic effect on RGCs (Hernandez *et al.*, 2010; Vecino *et al.*, 2015). Moreover, IOP

elevation caused by EVC model triggers an inflammatory response, activating microglia around ONH, which express proinflammatory cytokines (Roh *et al.*, 2012).

As described above, several animal models of RGC death and elevated IOP have been developed to try to unveil the mechanisms behind glaucomatous disease. In addition, *in vitro* models of EHP have been developed to evaluate cell responses at several timepoints and pressure levels (15 mmHg to 100 mmHg above atmospheric pressure) (Agar *et al.*, 2000; Agar *et al.*, 2006; Sappington *et al.*, 2009; Tok *et al.*, 2014). In the model of EHP, that we established in our laboratory, hydrostatic pressure levels are increased 70 mmHg above atmospheric pressure (Madeira *et al.*, 2015b). In fact, in the case of elevated IOP, some tissues in the eye are exposed to increased hydrostatic pressure: the retinochoroidal complex experiences increased hydrostatic pressure from within the vitreal chamber and from the suprachoroidal space, and RGC axons in the ONH are exposed continuously to increased hydrostatic pressure (Sappington *et al.*, 2009).

In models of EHP, it has been shown the induction of neuronal cell apoptosis, namely in RGCs (Madeira *et al.*, 2015b), and oxidative stress processes (Agar *et al.*, 2000; Agar *et al.*, 2006; Tok *et al.*, 2014). Moreover, submitting retinas or eye cup preparations to EHP induces glial cell activation, GFAP expression in Müller cells, and retinal axonal and Müller cell swelling (Ishikawa *et al.*, 2010; Ishikawa *et al.*, 2011). In the model that we used, which is similar to Sappington model, the increase of 70 mmHg above atmospheric pressure for 24h induces microglia reactivity and RGC death (Sappington *et al.*, 2009; Sappington *et al.*, 2010; Madeira *et al.*, 2015a).

#### **1.4. Cannabis and Endocannabinoids**

*Cannabis sativa*, the marijuana plant (Fig. 8), has as major active component,  $\Delta^9$ -tetrahydrocannabinol (THC), which is the main responsible for the psychoactive effects of cannabis consumption. Besides this effect, THC also produces numerous beneficial effects, including analgesia, appetite stimulation, nausea reduction and reduction of IOP. Due to these properties, cannabis has been used in medicine for decades (Pacher *et al.*, 2006; Pertwee, 2006). In addition, THC mimics the action of endogenous fatty acid derivatives, namely endocannabinoids (Yazulla, 2008).



**Figure 8** - *Cannabis sativa*, the marijuana plant (found in <http://www.medscape.com/viewarticle/837011>).

Endocannabinoids are neuromodulators in the CNS and act through two types of cannabinoid receptors: CB<sub>1</sub> and CB<sub>2</sub>. The most investigated endocannabinoids are N-arachidonylethanolamide (anandamide or AEA) and 2-arachidonoyl glycerol (2-AG), although many others are being studied, as palmitoylethanolamide (PEA) and oleoylethanolamide (OEA), 2-arachidonylglyceryl ether (noladin ether), oarachidonylethanolamine (virodhamine) and N-arachidonoyldopamine (Fig. 9).

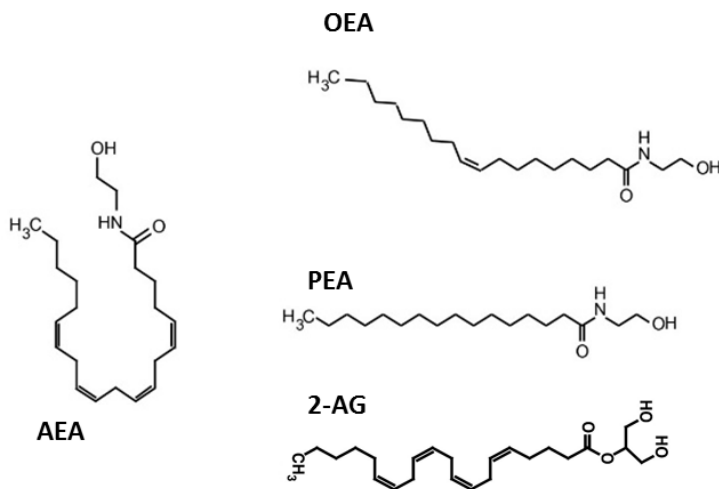


**Figure 9** - Chemical structures of the N-acylethanolamines: AEA – anandamide; PEA - palmitoylethanolamide; OEA – oleoylethanolamide; 2-AG - 2-arachidonoyl glycerol (adapted from (Joosten *et al.*, 2010) and from (Baur *et al.*, 2013)).

Furthermore, they belong to a very large group of bioactive lipids, which function as neuromodulators and immunomodulators. There is also evidence that endocannabinoids serve as retrograde synaptic messengers in the CNS (Pertwee, 2005; Vaughan and Christie, 2005; Yazulla, 2008).

Endocannabinoids have a role in neuroplasticity in several conditions, including pain, stroke, cancer, obesity, osteoporosis, fertility, neurodegenerative diseases, like glaucoma, and inflammatory diseases, among others (Yazulla, 2008). Moreover, several studies have demonstrated that endocannabinoids can have a neuroprotective effect in retinal cells (Nucci *et al.*, 2007). Also, it has been demonstrated that the endocannabinoid system is highly activated during CNS inflammation and that the endocannabinoid AEA protects neurons from inflammatory damage (Eljaschewitsch *et al.*, 2006;Hernangómez *et al.*, 2014).

#### 1.4.1. Endocannabinoid System

The endogenous cannabinoid system includes endocannabinoids, cannabinoid receptors, and the proteins involved in their biosynthesis, metabolism, and release. The two main endocannabinoids in the system are AEA and 2-AG, which are produced via a phospholipid-dependent pathway, released, and then taken up by cells via diffusion through the plasmatic membrane. Endocannabinoids are metabolized mostly via intracellular enzymatic hydrolysis. After their production, endocannabinoids are not accumulated into synaptic vesicles and are metabolized by fatty acid amide hydrolase (FAAH), in the case of AEA, and by monoacylglycerol lipase (MAGL) and FAAH, in the case of 2-AG (Di Marzo *et al.*, 2005) (Fig. 10).

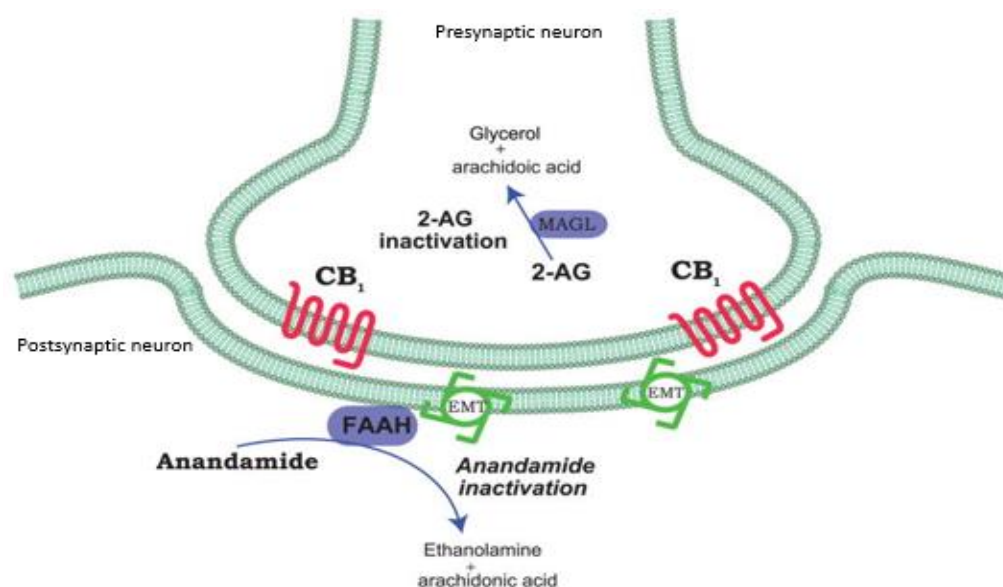


**Figure 10 - Endocannabinoid system in pre- and postsynaptic neurons.** The presynaptic terminal is located in the top, whereas the postsynaptic neuron is located in the bottom. The FAAH converts AEA in ethanolamide and arachidonic acid. The MAGL converts 2-AG into glycerol and arachidonic acid. FAAH - fatty acid amide hydrolase; EMT - endocannabinoid membrane transporter; MAGL - monoacylglyceride lipase (adapted from (Pacher *et al.*, 2006)).

The processes responsible for the production, membrane transport and enzymatic inactivation of endocannabinoids are all potential pharmacological targets, which can be modulated for experimental or therapeutic purposes. There is evidence that the modulation of the endocannabinoid system may also occur naturally as a result of the co-release of endogenous fatty acid derivatives such as PEA and OEA. These compounds can potentiate AEA effects and modulate endocannabinoid activity by competition at the receptors or by affecting substrate availability for metabolism (Di Marzo *et al.*, 2005; Yazulla, 2008). Furthermore, the inhibition of AEA metabolism by FAAH blockers increases the sensitivity of CB<sub>1</sub> or CB<sub>2</sub> receptors for AEA (Di Marzo *et al.*, 2005; Pertwee, 2005).

### 1.4.1.1. Endocannabinoid Receptors

Endocannabinoids act through two types of receptors: CB<sub>1</sub> receptors, localized predominantly in the CNS (Pertwee, 1997; Rivers and Ashton, 2010), and CB<sub>2</sub> receptors, localized mostly in the peripheral nervous system and are associated with mechanisms of the immune response (Tomida *et al.*, 2004; Rivers and Ashton, 2010).

CB<sub>1</sub> and CB<sub>2</sub> receptors are G<sub>i/o</sub> protein-coupled receptors that modulate the activity of several plasma membrane proteins and intracellular signaling pathways (Hernangómez *et al.*, 2014). Activation of both cannabinoid CB<sub>1</sub> and CB<sub>2</sub> receptors, and the subsequent stimulation of G<sub>i/o</sub> heterotrimeric proteins, leads to inhibition of adenylate cyclase (AC), and consequently to the inhibition of the protein kinase A (PKA) phosphorylation, or to stimulation of mitogen-activated protein kinase (MAPK) (Di Marzo *et al.*, 2004) (Fig. 11).

There are studies suggesting that CB<sub>1</sub> receptors affect different cellular functions depending if they are short-term or long-term activated. In one hand, activation for seconds of neuronal CB<sub>1</sub> receptors inhibits presynaptic voltage-activated calcium channels and activates inwardly rectifying potassium channels, reducing neurotransmission (Di Marzo *et al.*, 2004; Hernangómez *et al.*, 2014). On the other hand, CB<sub>1</sub> receptor activation for minutes to hours alter gene expression, for example, inducing the expression of neuroprotective proteins, such as brain-derived neurotrophic factor (BDNF), known to counteract cell damage (Hernangómez *et al.*, 2014) (Fig. 11).

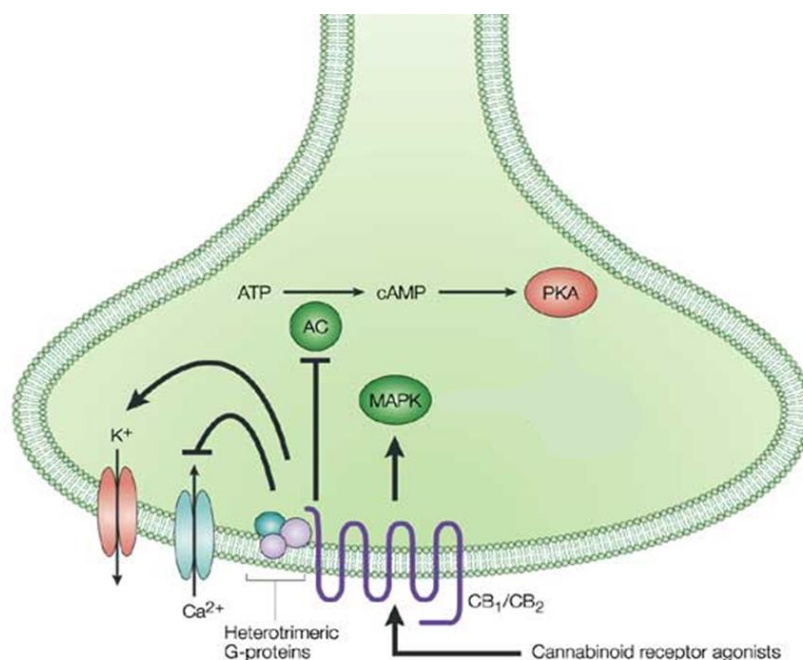


**Figure 11 – CB<sub>1</sub> and CB<sub>2</sub> receptors.** CB<sub>1</sub> and CB<sub>2</sub> receptors are G<sub>i/o</sub> protein-coupled receptors that when activated inhibit AC, thus modulating PKA phosphorylation or stimulating MAPK. AC - adenylyl cyclase; PKA - protein kinase A; MAPK - mitogen-activated protein kinase (adapted from (Di Marzo *et al.*, 2004)).

#### 1.4.2. Endocannabinoid System in the Eye

In the eye, marijuana and cannabinoids consumption produces hyperemia, due to local vasodilation, decreases intraocular pressure and changes retinal synaptic signalling (Yazulla, 2008;Slusar *et al.*, 2013). Furthermore, the presence of a functional endocannabinoid system localized in ocular tissues has been established (Hu *et al.*, 2010), and AEA and 2-AG have been detected in various ocular tissues, including retina (Yazulla, 2008). Also, the presence of the FAAH enzyme has been described in several structures of the eye, namely in the retina, choroid, iris, optic nerve and lacrimal gland (Matsuda *et al.*, 1997;Yazulla *et al.*, 1999). Moreover, as in the other tissues, FAAH in the eye is thought to be the primary mediator of the hydrolysis of released endocannabinoids (AEA, OEA and PEA). Enhancement of endocannabinoid responses can be achieved with inhibition of FAAH activity.

In the eye, CB<sub>1</sub> receptors are expressed in the ciliary body, iris, trabecular meshwork, and retina, mainly in the INL and GCL (Straiker *et al.*, 1999;Zhong *et al.*, 2005;Bouskila *et al.*, 2012). The ocular hypotensive effects of endocannabinoids might be related to their action on CB<sub>1</sub> receptors present in eye structures. However, it was also described the presence of CB<sub>2</sub> receptors in the trabecular meshwork and

its involvement in the IOP reduction mediated by endocannabinoids (Zhong *et al.*, 2005).

In summary, the endocannabinoid system has a role in ocular function and several findings have prompted considerable research into the therapeutic potential of targeting the endocannabinoid system for the treatment of a number of degenerative ocular diseases, including glaucoma (Nucci *et al.*, 2008).

### **I.4.3. URB597 and FAAH enzyme**

The FAAH inhibitor URB597 is carbamate inhibitor, which displays an excellent selectivity for FAAH in the nervous system, although the inhibitor does inactivate additional peripheral hydrolases (Mileni *et al.*, 2010). Furthermore, URB597 binds in the hydrophobic and catalytic core of FAAH that connects the active site residues to the membrane surface of FAAH (Mor *et al.*, 2004). It is described that URB597 reduces the expression of the LPS-induced enzymes cyclo-oxygenase 2 (COX-2) and iNOS in primary rat microglial cells, with a concomitant reduction in the release of the inflammatory mediators prostaglandin E<sub>2</sub> (PGE<sub>2</sub>) and NO (Tham *et al.*, 2007). Moreover, *in vivo* studies, URB597 inhibits anandamide hydrolysis in rat brain membranes and in parallel increase AEA, OEA and PEA levels in brain, by inhibition of FAAH (Fegley *et al.*, 2005). In addition, URB597 reduces allodynia and hyperalgesia through CB<sub>1</sub> and CB<sub>2</sub> receptors mediated analgesia in rats with inflammatory pain (Jayamanne *et al.*, 2006).

## 2. Aims

Glaucoma is a multifactorial neurodegenerative disease with complex genetic and environmental factors (Baltmr *et al.*, 2010), and elevated IOP is considered the major risk factor to develop glaucoma. In addition, growing evidence also indicates that neuroinflammation has a role in the pathophysiology of glaucoma, which is characterized by an increase in microglial reactivity and in the release of pro-inflammatory mediators (Madeira *et al.*, 2015a). All this together leads to damage of the optic nerve and loss of RGCs.

Both increased levels of FAAH enzyme, which degrades AEA, and elevated glutamate levels in the retina were reported in an acute experimental model of ocular hypertension (Nucci *et al.*, 2007). Moreover, increasing AEA levels, by inhibiting FAAH, reduced retinal damage in a model of optic nerve axotomy (Slusar *et al.*, 2013). Taken together, these evidences suggest that increasing local endocannabinoid levels, particularly AEA, may be an effective supplement to the arsenal of neuroprotective strategies for retinal neurodegenerative diseases, such as glaucoma. Moreover, taking into account the ocular hypotensive properties of endocannabinoids, in addition to its neuroprotective and anti-inflammatory effects, FAAH inhibitors have the potential to decrease IOP, thereby strengthening its relevance to treat glaucoma, protecting RGCs against degeneration.

One of the main goals of this project was to investigate for the first time the potential neuroprotective and anti-inflammatory effects of a FAAH inhibitor (URB597) in a model of EHP in rat retinal explants. Our preliminary results indicated that exposure of retinal explants to EHP increased endocannabinoids levels. Another goal was to assess the potential effect of URB597 in decreasing IOP in a model of ocular hypertension.

URB597 is a selective FAAH inhibitor with described neuroprotective and anti-inflammatory properties in only two studies in animal models: optic nerve axotomy model (Slusar *et al.*, 2013) and ischemia reperfusion model (Nucci *et al.*, 2007), which are not chronic glaucoma models. Therefore, the potential role of this compound in decreasing IOP in an animal model of hypertension is not clarified. In order to accomplish our goals, and to clarify whether the observed effects are mediated by CB<sub>1</sub> receptors activation by increased endocannabinoids levels, URB597 administered in the absence or presence of CB<sub>1</sub> antagonist (O-2050) to animals submitted to EVC, to evaluate its effect on IOP. Similarly, retinal explants were challenged with EHP and were pre-incubated with URB957, in the absence or presence O-2050. In retinal

## Aims

explants, it was evaluated FAAH activity, levels of endocannabinoids, alterations in the morphology of microglial cells, iNOS expression in microglia, nitric oxide and pro-inflammatory cytokines production, and RGC death.

# CHAPTER 3

---

*Methods*



### 3. Methods

#### 3.1.1. Animals

Male Wistar Han rats were housed under controlled environment ( $22 \pm 0.1^\circ\text{C}$  of temperature,  $67.6 \pm 1.6\%$  of relative humidity, 12 h-light/dark cycle) and were maintained in a food and water *ad libitum* regime.

All procedures involving animals were in accordance with European Community guidelines for the use of animals in laboratory (Directive 2010/63/EU) and in accordance with the “Association for Research in Vision and Ophthalmology (ARVO)” rules for the use of animals in ophthalmology and vision science experimentation.

#### 3.1.2. Retinal Organotypic Cultures

Animals aged 8-10 weeks were sacrificed by cervical dislocation. The eyes were enucleated and dissected in sterile  $\text{Ca}^{2+}$ - and  $\text{Mg}^{2+}$ -free HBSS (in mM: 132 NaCl, 5.4 KCl, 0.45  $\text{KH}_2\text{PO}_4$ , 0.45  $\text{Na}_2\text{HPO}_4$ , 4  $\text{NaHCO}_3$ , 2.8 glucose, 5 HEPES, pH 7.3). The obtained retinal explants were flat-mounted onto 30 mm diameter culture plate inserts with a  $0.4 \mu\text{m}$  pore size (Millicell, Millipore, USA), with the GCL facing up (Fig. 12). Explants were then cultured in 6-well plates containing Dulbecco’s modified Eagle medium: Nutrient Mixture F-12 (DMEM/F-12) medium containing GlutaMAX I (Life Technologies, USA), supplemented with 10% fetal bovine serum (FBS; Life Technologies, USA) and 0.1% gentamicin (Life Technologies). Retinal explants were maintained for 3 days *in vitro* (DIV) in a humidified incubator at  $37^\circ\text{C}$  with 5%  $\text{CO}_2$ . At DIV1 and DIV2, culture medium was replaced with fresh medium.

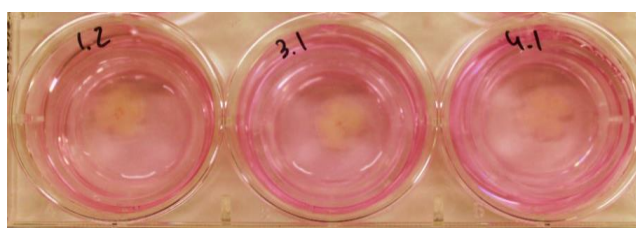


**Figure 12** - Retinal organotypic culture at DIV0 with the RGC facing up.

#### 3.1.3. Drug Exposure to Retinal Organotypic Cultures

Retinal explants were incubated at DIV2 with  $10 \mu\text{M}$  URB597 (FAAH inhibitor; Sigma-Aldrich, USA). After 1 h of incubation, retinal explants were exposed to EHP ( $+70 \text{ mmHg}$  above atmospheric pressure; Fig. 13) for 24 h. In some retinal explants,

## Methods

a pre-treatment with 10  $\mu$ M O-2050 (CB<sub>1</sub> receptor antagonist; Tocris, UK), was applied 15 min before incubation with URB597 (Fig. 14).



**Figure 13** – Pressure chamber. Humidified pressure chamber, equipped with a regulator to ensure +70 mmHg, placed inside an oven at 37°C.

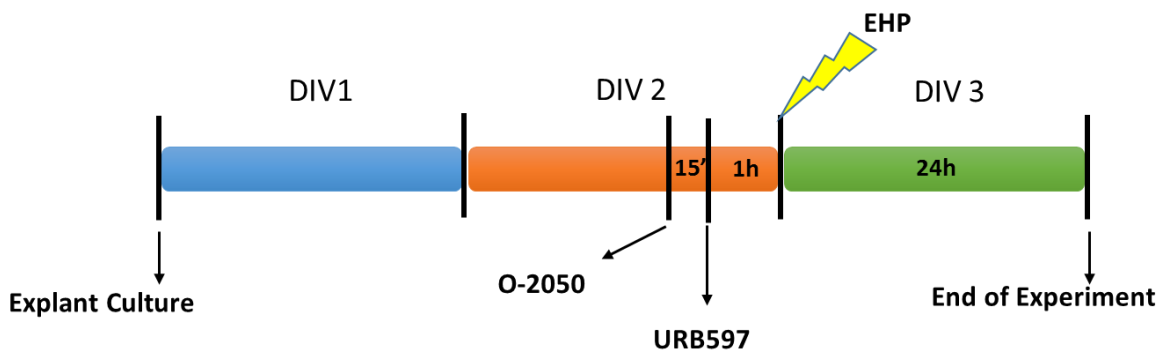


**Figure 14** - Schematic representation of drug exposure in retinal explant cultures.

### 3.1.4. Immunohistochemistry

Retinal explants were washed three times with warmed phosphate buffered saline (PBS, in mM: 137 NaCl, 2.7 KCl, 10 Na<sub>2</sub>HPO<sub>4</sub>, 1.8 KH<sub>2</sub>PO<sub>4</sub>, pH 7.4) solution and fixed with ice-cold 100% ethanol for 10 min at 4°C. Explants were washed again with PBS, and non-specific binding was prevented by incubation with 3% bovine serum albumin (BSA), 10% normal goat serum (NGS), and 0.1% Triton X-100, in PBS, for 1 h at room temperature (RT). Samples were then incubated with primary antibodies (Table I) in blocking solution for 48 h at 4°C. After being washed several times with PBS, explants were incubated with secondary antibodies (Table I) overnight (o.n.) at 4°C in the dark. Then, explants were extensively washed with PBS and incubated with DAPI (1:1000; Life Technologies, USA) for 15 min in the dark to stain nuclei. After washing,

explants were flat-mounted on glass slides with the GCL facing upwards and coverslipped with Glycergel mounting medium (Dako, Denmark). The images were acquired in a laser scanning confocal microscope LSM 710 (Zeiss, Germany).

**Table 1** – List of primary and secondary antibodies used in the immunohistochemistry

	Supplier (cat no)	Host	Dilution
<b>Primary Antibodies</b>			
Anti-Brn3a	Chemicon (MAB1585)	Mouse	1:500
Anti-CD11b	Serotec (MCA275G)	Mouse	1:100
Anti-iNOS	Santa Cruz Biotechnology (NOS2M-19)	Rabbit	1:200
<b>Secondary Antibodies</b>			
Alexa Fluor® 488 Anti-Rabbit IgG	Invitrogen (A11008)	Goat	1:200
Alexa Fluor® 568 Anti-Mouse IgG	Invitrogen (A11004)	Goat	1:200

### 3.1.5. TUNEL Assay

TdT-mediated dUTP nick-end labeling (TUNEL) assay was performed according to instructions provided by the manufacturer (Promega, USA).

Retinal explants were fixed with ice-cold 100% ethanol for 10 min at 4°C, and then hydrated twice with PBS. Samples were permeabilized with 20 µg/mL proteinase K for 15 min at RT, followed by incubation with equilibration buffer (200 mM potassium cacodylate, 25 mM Tris-HCl, 0.2 mM DTT, 0.25 mg/mL BSA and 2.5 mM cobalt chloride) for 10 min. Explants were then incubated with the recombinant TdT enzyme and nucleotide mix containing dUTP conjugated with fluorescein, at 37°C for 1 h. The reaction was stopped by incubating the explants in saline-citrate buffer for 15 min at RT and then washed three times for 5 min with PBS. The nuclei were stained with DAPI (1:1000; Life Technologies). After washing, retinal explants were flat-mounted on glass slides with the GCL facing upwards and coverslipped with Glycergel mounting medium (Dako). The images were acquired in a laser scanning confocal microscope LSM 710 (Zeiss).

### 3.1.6. Image Analysis

Immunostained retinal explants were examined in a Zeiss LSM 710 confocal microscope. For each condition, 4 images per quadrant, in a total of 16 images, were acquired randomly with a Plan-Apochromat 20x/0.8 M27 objective lens. In order to compare the different conditions, all images were acquired using the same gain and exposure settings.

Densitometric analysis was performed for iNOS/CD11b stained cells using the public domain ImageJ program (<http://rsb.info.nih.gov/ij/>). The immunoreactivity of each cell was calculated using the following formula, as previously described (Gavet and Pines, 2010):

Corrected total cell fluorescence = Integrated density – (Area of selected cell x Mean fluorescence of background readings).

To assess differences in microglial morphology, the particle measurement feature in ImageJ was used to calculate the 2D area, perimeter, circularity, and Feret's diameter of each microglial cell present in each image collected. As previously described (Kurpius *et al.*, 2006), threshold was uniformly set to outline microglial cells and the four parameters were then automatically measured. Circularity was evaluated using the following formula:

$$\text{circularity} = 4\pi(\text{area}/\text{perimeter}^2)$$

A circularity value of 1.0 indicates a perfect circular cell, and as the value approaches 0, it indicates increasingly ramified cells. Feret's diameter is a measure of the cell's length. It represents the longest distance between any two points along the selection boundary.

### 3.1.7. Endocannabinoid Levels in Retinal Explants

The levels of the endocannabinoids anandamide (AEA), oleoylethanolamide (OEA), and palmitoylethanolamide (PEA) in retinal organotypic cultures were analyzed by liquid chromatography coupled with tandem mass spectrometry (LC-MS/MS) at BIAL laboratories. Samples were collected and immediately stored at -80°C, and then shipped to BIAL for posterior analysis.

#### Sample preparation for LC-MS/MS analysis

Frozen explants previously weighed were homogenized in 500 µL of

chloroform:methanol (2:1) and 500  $\mu\text{L}$  of 0.1 M phosphate buffer, pH 5.6. Tissue homogenates were spiked with 1  $\mu\text{L}$  of 125  $\mu\text{g}/\text{mL}$  internal standard (AEA-d8, PEA-d4, OEA-d2). Samples were then subjected to chloroform:methanol extraction. After centrifugation, the organic layer was carefully removed and transferred to a plastic vial. The aqueous layer was re-extracted with 500  $\mu\text{L}$  of chloroform:methanol (2:1). This procedure was repeated twice and the organic layer was combined and evaporated in a speed-vacuum at 35°C to dryness. The samples were reconstituted with 100  $\mu\text{L}$  of acetonitrile and injected into LC-MS/MS to measure the fatty acids.

### 3.1.8. Evaluation of FAAH Activity in Retinal Explants

FAAH activity in retinal explants was also measured at BIAL laboratories. Retinal explants were collected in vials containing 750  $\mu\text{L}$  of membrane buffer (3 mM  $\text{MgCl}_2$ , 1 mM EDTA, 50 mM Tris-Cl, pH 7.4). Samples were stored immediately at -80 °C and then shipped to BIAL for posterior analysis.

#### Sample preparation

Frozen explants previously weighed were homogenized with homogenizer Precellys 24 (Bertin, France) using ceramic beads. Total protein content in tissue homogenates was determined with the BioRad protein assay (BioRad, USA) using a standard curve of BSA (50-250  $\mu\text{g}/\text{mL}$ ).

#### Reagents and solutions

Anandamide [ethanolamine-1- $^3\text{H}$ , AEA] was obtained from American Radiochemicals with a specific activity of 60 Ci/mmol (batch 140320). All other reagents were obtained from Sigma-Aldrich. Optiphase Supermix was obtained from Perkin Elmer.

#### FAAH activity determination

Reaction mix (total volume of 200  $\mu\text{L}$ ) contained: the substrate AEA (ratio cold:hot 400:1, 2  $\mu\text{M}$  AEA + 5 nM  $^3\text{H}$ -AEA), 0.1% fatty acid free BSA, 60  $\mu\text{g}$  protein, in 1 mM EDTA, 10 mM Tris, pH 7.6. After 15 min of pre-incubation at 37°C the reaction was started by the addition of the substrate solution (cold AEA + radiolabelled AEA + BSA). The reaction was carried out for 25 min at 37°C and terminated by addition of 400  $\mu\text{L}$  activated charcoal suspension (8 g charcoal in 32 mL 0.5 M HCl in continuous

agitation). After a 30 min incubation period at RT with agitation, charcoal was sedimented by centrifugation in a microfuge (10 min at 13000 rpm). Then, 200  $\mu$ L of supernatants were added to 800  $\mu$ L Optiphase Supermix scintillation cocktail previously distributed in 24-well plates. Counts per minute (CPM) were determined in a Microbeta TriLux scintillation counter (PerkinElmer, USA) (10 min counting). In each assay, blank samples (without protein) were prepared.

### **3.1.9. Animal Training and Handling**

The values of IOP may vary due to several factors, such as the time of the day (Gelatt and MacKay, 1998), animal stress (Miyazaki *et al.*, 2000), and anesthesia (Murphy, 1985). Therefore, to reduce the stress of animals and the potential effects of anaesthetics on IOP, all animals were handled to become accustomed to the researcher and to the tonometer. A training paradigm was implemented, which consisted in the following protocol: before starting the experiments, animals were trained for 2 weeks. During the first 3 days, the animals were acclimatized to the experimental room and to the technician who handled the animals. Also, animals were habituated to corneal touch (technician fingers, with gloves). In the following days, the animals were accustomed to IOP measurements with the Tonolab tonometer (iCare, Finland). Animals were also accustomed to restraint for drug administration.

In the period of handling and training, several factors were taken into account: the training/measurements were performed in the same period of the day (to avoid circadian variations in IOP); before handling the animals, they were acclimatized to the room for 15-20 min; between each measurement the benches were cleaned with 70% ethanol; the animal bedding was changed twice a week, but only after the training/measurements; the animals were weighed every week and 1 or 2 days before the experiments.

### **3.1.10. IOP Measurements**

IOP was measured with the Tonolab tonometer. This tonometer was specially designed to measure IOP in rodents (Morrison *et al.*, 2009). In order to decrease variability and increase IOP measurement confidence, 10 IOP readings were performed for each eye, always starting by the right eye. IOP measurements were performed immediately before drug administration and at the timepoints indicated in the figure 16.

The IOP measurements of the last 3 days of training were considered as basal values of reference.

### 3.1.1.1. Animal Model of Ocular Hypertension

After two weeks of animal training, ocular hypertension was induced in animals, by decreasing the outflow of aqueous humour from the anterior chamber. This was achieved by episcleral vein cauterization (Shareef *et al.*, 1995;Urcola *et al.*, 2006). Both eyes of each animal were submitted to interventions.

Animals were anesthetized with 2.5% isoflurane (Abbott Laboratories, USA), and 4 mg/mL oxybuprocaine (Anestocil, Edol) was topically applied in the eye to minimize animal distress. Episcleral veins were exposed by a conjunctival incision, after lateral canthotomy. Two of the episcleral veins that are dorsally positioned, near to the superior rectus muscle, and another vein that is temporally positioned close to the lateral rectus muscle, were isolated from the involving tissues (Fig. 15). Then, a low-temperature ophthalmic cautery (World Precision Instruments, USA) was used to cauterize the veins, taking care to avoid damaging the surrounding tissue. In the final procedure, a viscous eye drops containing fusidic acid (10 mg/g, Fucithalmic, LEO Pharmaceuticals, Denmark) was applied.

IOP was measured before (basal values) and daily after the procedure. Only the eyes with an IOP above 16 mmHg and with 30% increase above basal IOP values were considered with ocular hypertension and were used in the subsequent experiments.

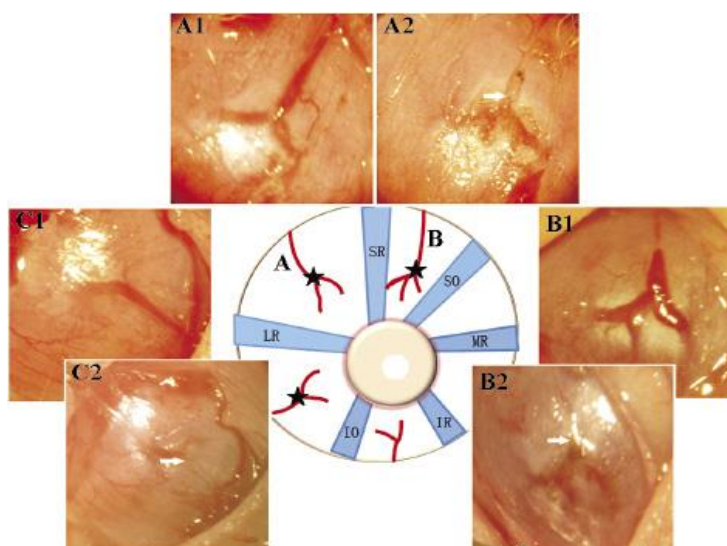


**Figure 15** - Scheme of the episcleral vein localization in the eyeball. A1, B1, and C1: episcleral veins before cauterization; A2, B2, and C2: episcleral veins after being cauterized. SR- superior rectus muscle; LR - lateral rectus muscle; SO - superior oblique muscle; IO - inferior oblique muscle; IR - inferior rectus muscle and MR – medial rectus muscle (adapted from (Bai *et al.*, 2014)).

### 3.1.12. Drug Preparation and administration to animals with or without ocular hypertension

Stock solution of FAAH inhibitor, URB597, was prepared in dimethyl sulfoxide (DMSO), as indicated by the supplier, and kept at  $-20^{\circ}\text{C}$ . URB597 and O-2050 emulsion were prepared in Tocrisolve 100 (1:4 ratio of soya oil/water, which was emulsified with the block co-polymer, Pluronic F68; Tocris, UK) in the day of the experiment.

URB597 and O-2050 were administered separately by intraperitoneal injection (i.p.) in the dose of 10 mg/kg and 1 mg/kg, respectively. Control animals received a single i.p. injection of vehicle (Tocrisolve).

Animals were randomly divided into 7 experimental groups, 4 groups with elevated IOP and 3 groups without elevated IOP. IOP was measured immediately before drug administration ( $t=-2$  h). URB597 or vehicle (Tocrisolve) were administered (i.p.) at the initial time point ( $t=-2$  h). O-2050 or vehicle were administered (i.p.) 1 h after URB597 administration, at  $t=-1$  h. IOP was measured after drug administration at the following timepoints:  $t=0$  h,  $t=2$  h and  $t=3$  h (Fig. 16).

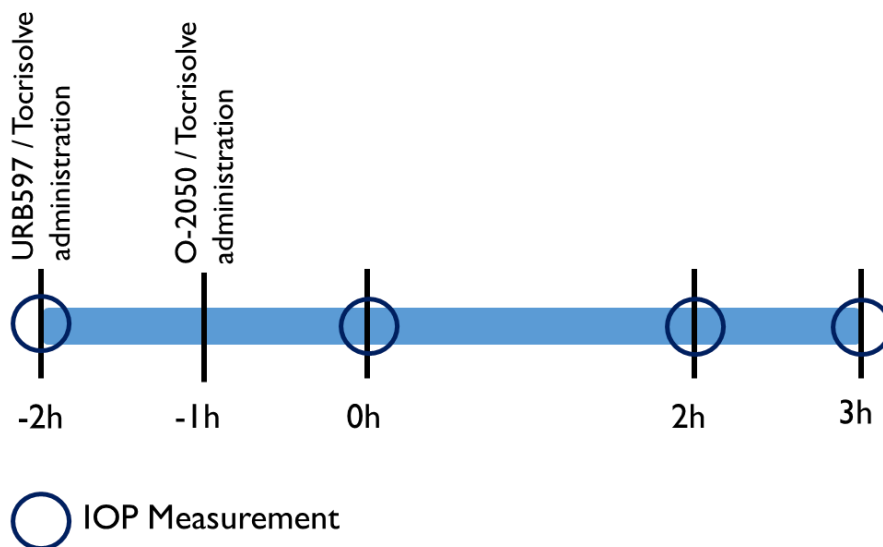


**Figure 16-** Scheme of drug administration and IOP measurements.

### 3.1.13. Statistical Analysis

Results are presented as mean  $\pm$  standard error of the mean (SEM). Statistical analysis was performed using GraphPad Prism (GraphPad Software, USA). Differences were considered statistically significant for  $p < 0.05$ .

In the results obtained from tasks using retinal explants, parametric One Way

ANOVA test was used, followed by Holm-Sidak's multiple comparison test.

To analyse differences in IOP between control and EVC animals, until 7 days of inducing elevated IOP by episcleral vein cauterization, the statistical significance was evaluated with parametric Two Way ANOVA test, followed by Sidak's multiple comparisons test.

In tasks using animals administrated with drugs, IOP values were normalized according to the following formula:

$$\text{IOP}(t_x) = \frac{\text{IOP}(t_x) - \text{IOP}(t_i)}{\text{IOP}(t_i)}, t_i = -2 \text{ h.}$$

In this case, the statistical significance was evaluated with parametric Two Way ANOVA test, followed by Tukey's multiple comparison test, to compare the effects of drugs with the vehicle, as well as to compare the effects of drugs, at the same timepoint. To analyse the drug effect along time, Repeated Measurements One Way ANOVA was used, followed by Tukey's multiple comparison test.



# CHAPTER 4

---

*Results*



## 4. Results

In the present work, one of the main goals was to evaluate whether URB597, a selective inhibitor of FAAH, could be able to decrease the IOP in an animal model of ocular hypertension. Therefore, 7 days after performing EVC in the animals, URB597 was injected intraperitoneally. To evaluate whether the potential effect of URB597 could be mediated, at least partially, by CB<sub>1</sub> receptors, in some experiments, O-2050, a CB<sub>1</sub> receptor antagonist, was administered (i.p.) 1 h after URB597. IOP was measured immediately before and 2 h, 4 h, and 5 h after URB597 administration. Another goal was to investigate whether URB597 could have neuroprotective and anti-inflammatory effects in rat retinal explants subjected to elevated hydrostatic pressure (EHP). As in the EVC animal model, in retinal explants it was also intended to investigate whether the effects of URB597 could be mediated by CB<sub>1</sub> receptor activation. For this purpose, retinal explants were challenged with EHP and were pre-incubated with URB597, in the absence or presence of O-2050.

### 4.1. Effect of EVC on IOP

IOP was measured during 7 days in control animals (without EVC) and in animals submitted to EVC (Fig. 17). After EVC procedure, there was a significant increase in IOP comparing to control animals, in all days analysed. At day 1, the IOP value in EVC animals was  $17.7 \pm 1.9$  mmHg, significantly higher compared with control animals ( $13.5 \pm 0.5$  mmHg). At day 7, the IOP in EVC animals was  $18.6 \pm 0.6$  and in control animals was  $13.3 \pm 0.6$  mmHg.

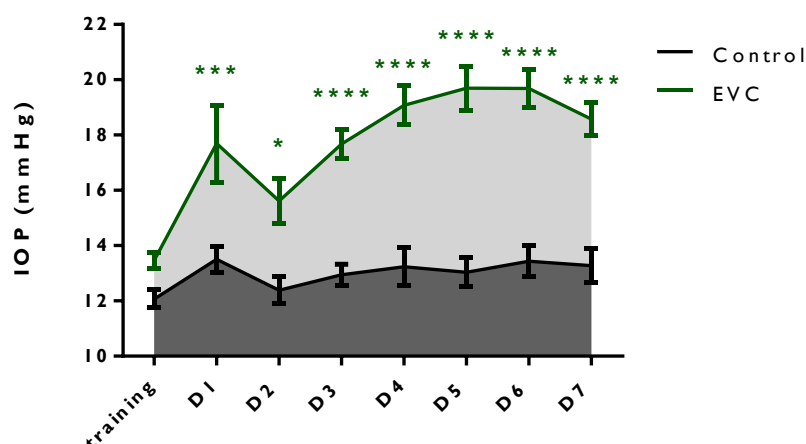


**Figure 17 - EVC increases IOP for 7 days.** In animals subjected to EVC, the cauterization was performed in both eyes. The data represent the average IOP values in each eye of 6 - 8 animals, in each day, during 7 days after EVC procedure. \* $p < 0.05$ , \*\*\* $p < 0.001$ , and \*\*\*\* $p < 0.0001$ , significantly different compared with control, Two-way ANOVA followed by Sidak's multiple comparisons test.

#### 4.2. Effect of URB597 and O-2050 administration in IOP in animals with and without ocular hypertension

It was evaluated the effect of URB597 (FAAH inhibitor) in IOP of animals submitted to EVC model, and if this effect would be mediated by CB<sub>1</sub> receptor activation.

It was observed that there were no significant changes with the vehicle treatment in animals with or without ocular hypertension (EVC model) (Fig. 18), in IOP along the several time points. Similarly, in control animals, URB597 (10 mg/kg, i.p.) or O-2050 (1 mg/kg, i.p.) administration had no significant alterations in IOP along time (Fig. 19). In animals with ocular hypertension, the administration of O-2050 did not alter IOP at the different time points (Fig. 20). However, URB597 treatment significantly decreased the IOP (Figs. 21 and 22) in animals with ocular hypertension at the time points  $t=2$  h and  $t=3$  h ( $p<0.05$ ), as well as comparing with the control condition at the time points  $t=2$  h ( $p<0.05$ ) and  $t=3$  h ( $p<0.01$ ), and compared with the initial time point ( $t=-2$  h), at  $t=2$  h ( $p<0.01$ ) and  $t=3$  h ( $p<0.001$ ). When the CB<sub>1</sub> receptor antagonist, O-2050, was administered to animals with EVC that were pre-treated with URB597, the effect of URB597 was significantly inhibited at the time point  $t=3$  h ( $p<0.05$ ). Moreover, in the same group of animals, at the time point  $t=0$  h, there was a significant decrease ( $p<0.05$ ) of IOP compared with initial time point ( $t=-2$  h), although this appears to be a common trend in all groups (Fig. 22).

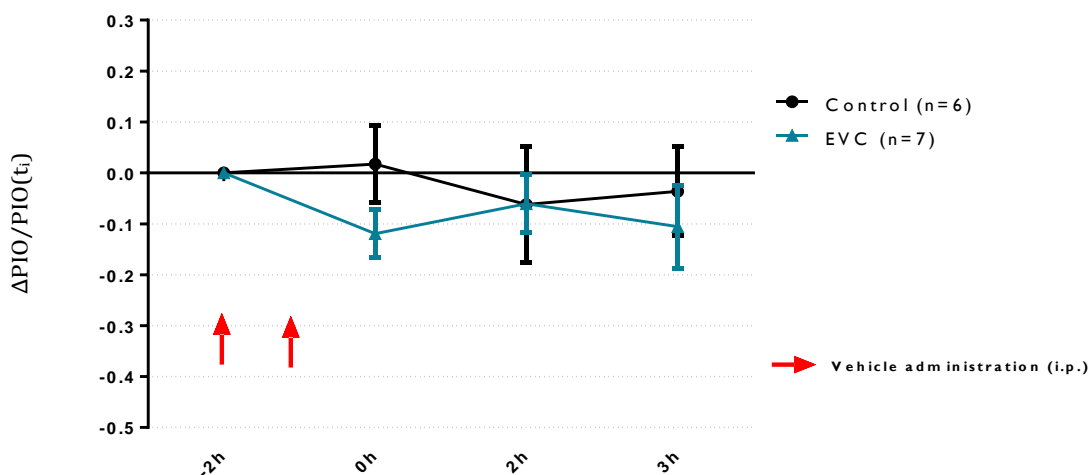


**Figure 18 - Evaluation of the potential effect of vehicle administration in the IOP of animals with and without ocular hypertension (EVC model).** Vehicle (Tocrisolve) was administered at  $t=-2$  h and at  $t=-1$  h. IOP was measured at the time points  $t=-2$  h,  $t=0$  h,  $t=2$  h, and  $t=3$  h. The results are expressed as mean  $\pm$  SEM of the values calculated according to the formula described in the statistical analysis section. The number of animals is indicated between brackets.

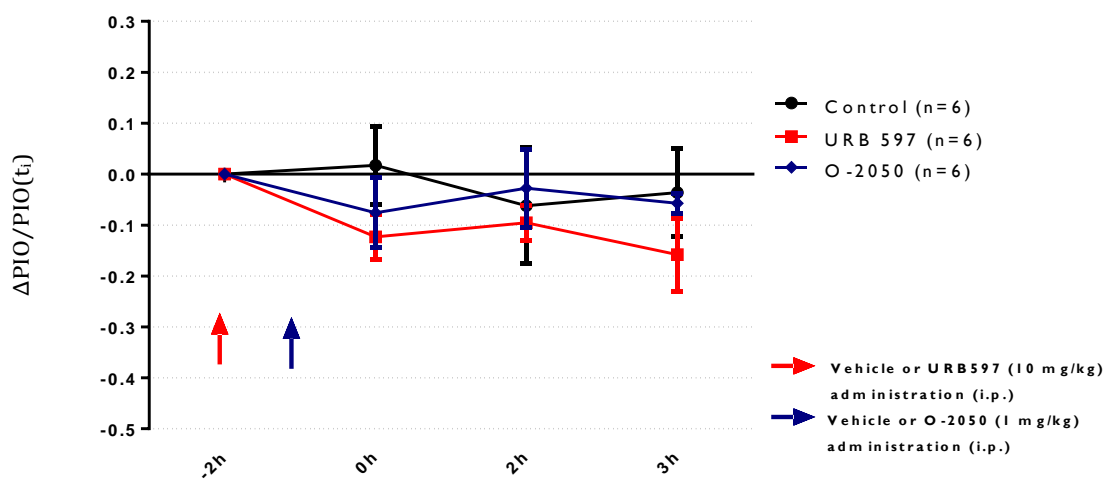


**Figure 19 - Evaluation of the potential effect of FAAH inhibitor, URB597, or CB<sub>1</sub> receptor antagonist, O-2050, in the IOP of control animals with normal IOP.** URB597 (10 mg/kg) or vehicle (Tocrisolve) were administered at  $t=-2$  h, and O-2050 (1 mg/kg) or vehicle (Tocrisolve) were administered at  $t=-1$  h. IOP was measured at the time points  $t=-2$  h,  $t=0$  h,  $t=2$  h, and  $t=3$  h. The results are expressed as mean  $\pm$  SEM of the values calculated according to the formula described in the statistical analysis section. The number of animals is indicated between brackets.

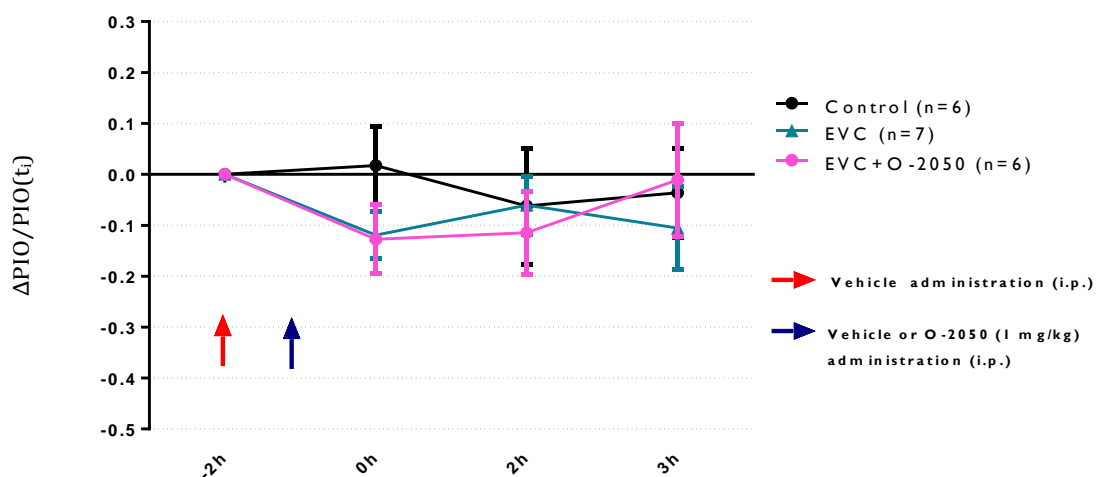


**Figure 20 - Evaluation of the potential effect of CB<sub>1</sub> receptor antagonist, O-2050, in the IOP of animals with ocular hypertension (EVC model).** O-2050 (1 mg/kg) was administered at  $t=-1$  h, and vehicle (Tocrisolve) was administered at  $t=-2$  h and at  $t=-1$  h. IOP was measured at the time points  $t=-2$  h,  $t=0$  h,  $t=2$  h, and  $t=3$  h. The results are expressed as mean  $\pm$  SEM of the values calculated according to the formula described in the statistical analysis section. The number of animals is indicated between brackets.

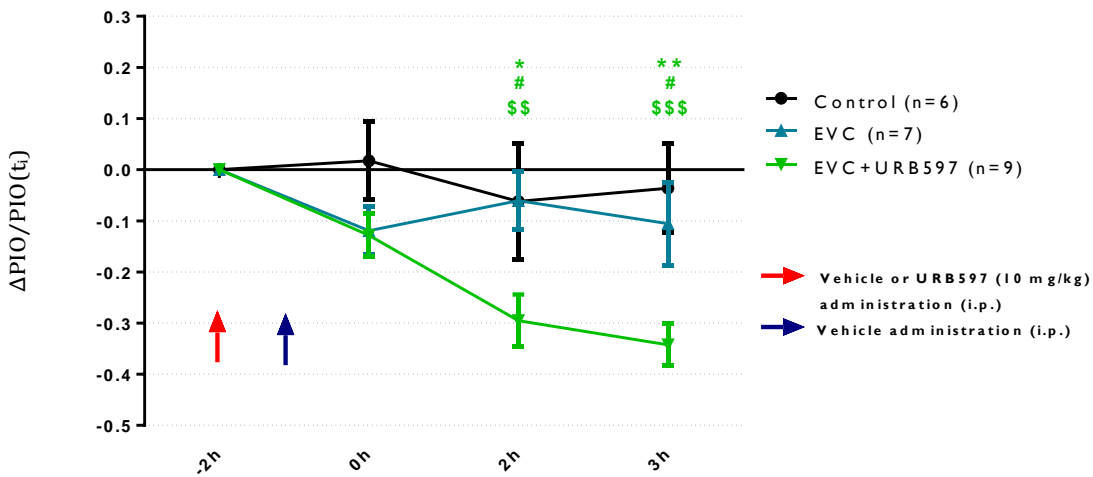


**Figure 21 - Evaluation of the effect of FAAH inhibitor, URB597, in the IOP of animals with ocular hypertension (EVC model).** URB597 (10 mg/kg) was administered at  $t=-2$  h, and vehicle (Tocrisolve) was administered at  $t=-2$  h and at  $t=-1$  h. IOP was measured at the time points  $t=-2$  h,  $t=0$  h,  $t=2$  h, and  $t=3$  h. The results are expressed as mean  $\pm$  SEM of the values calculated according to the formula described in the statistical analysis section. The number of animals is indicated between brackets. \* $p<0.05$ , \*\* $p<0.01$ , compared with control; # $p<0.05$ , compared with EVC; Two-way ANOVA followed by Tukey's multiple comparisons test. \$\$ $p<0.01$  and \$\$\$ $p<0.001$ , compared with  $t=-2$  h; Repeated Measurements One Way ANOVA followed by Tukey's multiple comparisons test. .

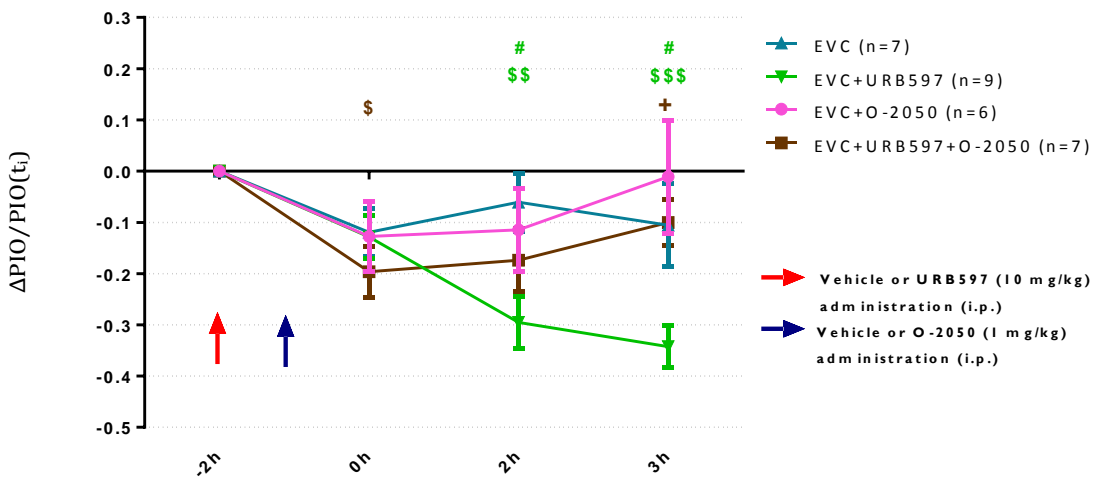


**Figure 22 - Evaluation of the effect of the CB<sub>1</sub> receptor antagonist, O-2050, on the reduction of IOP triggered by the FAAH inhibitor, URB597, in animals with ocular hypertension (EVC model).** URB597 (10 mg/kg) or vehicle (Tocrisolve) were administered at  $t=-2$  h and O-2050 (1 mg/kg) or vehicle (Tocrisolve) were administered at  $t=-1$  h. IOP was measured at the time points  $t=-2$  h,  $t=0$  h,  $t=2$  h, and  $t=3$  h. The results are expressed as mean  $\pm$  SEM of the values calculated according to the formula described in the statistical analysis section. The number of animals is indicated between brackets. # $p<0.05$ , compared with EVC; + $p<0.05$ , compared with EVC+URB597; Two-way ANOVA followed by Tukey's multiple comparisons test. \$ $p<0.05$ , \$\$ $p<0.01$ , \$\$\$ $p<0.001$ , compared with  $t=-2$  h; Repeated Measurements One Way ANOVA followed by Tukey's multiple comparisons test.

### 4.3. URB597 inhibits FAAH activity in retinal explants

The hydrolysis of endocannabinoids occurs mainly by FAAH, and enzyme that has been found in ocular tissues, including the retina (Matsuda *et al.*, 1997; Yazulla *et al.*, 1999). Since we aimed to evaluate the effect of FAAH inhibition on retinal explants, it was used URB597, a selective FAAH inhibitor (Slusar *et al.*, 2013). Thus, it was measured the FAAH activity in control retinal explants and in retinal explants exposed to EHP, untreated or treated with URB597 (Fig. 23). In control, the FAAH activity was  $19375 \pm 1284$  counts per minute (CPM). Exposure to EHP did not significantly alter FAAH activity ( $106.0 \pm 3.8$  % of control). As expected, in retinal explants treated with URB597, FAAH activity significantly decreased to  $0.09 \pm 0.03$  % of control or  $0.17 \pm 0.07$  % of EHP ( $p < 0.0001$ ).

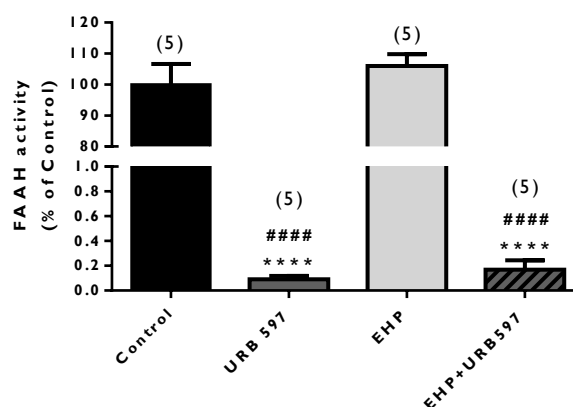


**Figure 23 - URB597 inhibits FAAH activity in retinal explants.** Retinal explants were cultured for 3 days and challenged, or not, with elevated hydrostatic pressure (EHP) at day 2 in culture, for 24 h, in the absence or presence of  $10 \mu\text{M}$  URB597 (FAAH inhibitor). The results are expressed in percentage of control as mean  $\pm$  SEM. The number of independent experiments is indicated above the bars. \*\*\*\* $p < 0.0001$ , compared with control; #### $p < 0.0001$ , compared with EHP; One-way ANOVA followed by Holm-Sidak's multiple comparisons test.

### 4.4. URB597 increases endocannabinoids levels in retinal explants

In mammals, AEA, PEA and OEA, are synthesized from glycerophospholipids and are degraded by FAAH (Ueda *et al.*, 2013). Therefore, we aimed to evaluate whether the inhibition of FAAH by URB597, in retinal explants, as shown above, could increase the endocannabinoid levels in retinal explants exposed, or not, to EHP.

In control condition, the AEA levels was  $21.84 \pm 2.51$  ng/g (Fig. 24A). Exposure to EHP *per se* did not significantly alter AEA levels, ( $24.3 \pm 3.09$  ng/g). In retinal explants under normal pressure conditions treated with URB597, AEA levels increased

## Results

significantly to  $530 \pm 95.1$  ng/g, comparing to control ( $p < 0.01$ ). In retinal explants challenged with EHP and treated with URB597 the AEA levels also significantly increased to  $916.6 \pm 170.8$  ng/g, comparing with EHP ( $p < 0.0001$ ), and compared with URB597 condition ( $p < 0.05$ ).

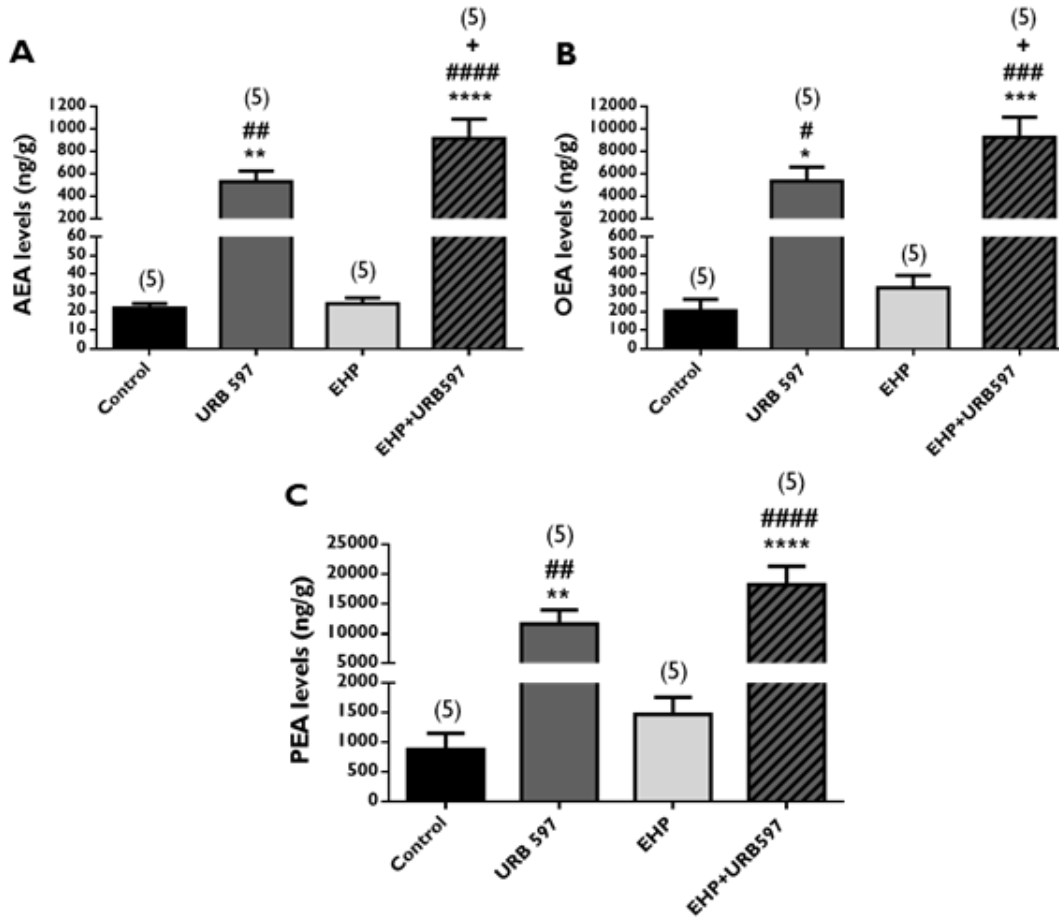


**Figure 24 – URB597 increases the levels of endocannabinoids in retinal explants.** The levels of AEA (A), OEA (B), and PEA (C) were measured in retinal explants cultured for 3 days and challenged, or not, with EHP, at day 2 in culture, for 24 h, in the absence or presence of 10  $\mu$ M URB597 (FAAH inhibitor). The results are expressed as mean  $\pm$  SEM. The number of independent experiments is indicated above the bars. \* $p < 0.05$ , \*\* $p < 0.01$ , \*\*\* $p < 0.001$ , \*\*\*\* $p < 0.0001$ , compared with control; # $p < 0.05$ , ## $p < 0.01$ , ### $p < 0.001$ , #### $p < 0.0001$ , compared with EHP; \* $p < 0.05$ , compared with URB597; One-way ANOVA followed by Holm-Sidak's multiple comparisons test.

Relatively to OEA levels (Fig. 24B), in control the concentration was  $203.6 \pm 62.6$  ng/g. When explants were exposed to EHP, there was no significant alteration in OEA levels ( $327.1 \pm 66.7$  ng/g), similarly to what was found for AEA levels. Treatment with URB597 increased significantly OEA levels ( $5361 \pm 1245$  ng/g), comparing with the control ( $p < 0.05$ ). In explants exposed to EHP, URB597 also increased significantly OEA levels ( $9277 \pm 1800$  ng/g), comparing with explants in control condition

( $p < 0.001$ ), exposed to EHP ( $p < 0.001$ ), and comparing with explants under normal pressure exposed to URB597 ( $p < 0.05$ ).

Regarding PEA levels (Fig. 24C), in the control condition, the concentration was  $881.6 \pm 270.9$  ng/g. Exposure to EHP *per se* did not significantly alter PEA levels ( $1470 \pm 286.6$  ng/g), similarly to what happened with the other two endocannabinoids. In retinal explants under normal hydrostatic pressure conditions treated with URB597, PEA levels increased significantly ( $11665 \pm 2337$  ng/g), comparing with the control ( $p < 0.01$ ). In retinal explants challenged with EHP and treated with URB597, PEA levels also increased significantly ( $18251 \pm 3103$  ng/g), comparing with EHP ( $p < 0.0001$ ). Thus, in retinal explants, FAAH inhibition increases endocannabinoid levels.

#### 4.5. Evaluation of the effect of FAAH inhibitor on apoptotic cell death in retinal explants

It was evaluated whether exposure of retinal explants to URB597 could induce cell death, particularly in the RGC layer. To accomplish this goal, was performed TUNEL assay in retinal explants (Fig. 25A). Was observed that URB597 ( $10 \mu\text{M}$ ) did not significantly alters the number of TUNEL positive cells in RGC layer ( $136.6 \pm 12.7$  % of control) compared with control. Thus, the inhibition of FAAH did not induce apoptotic cell death in the RGC layer.

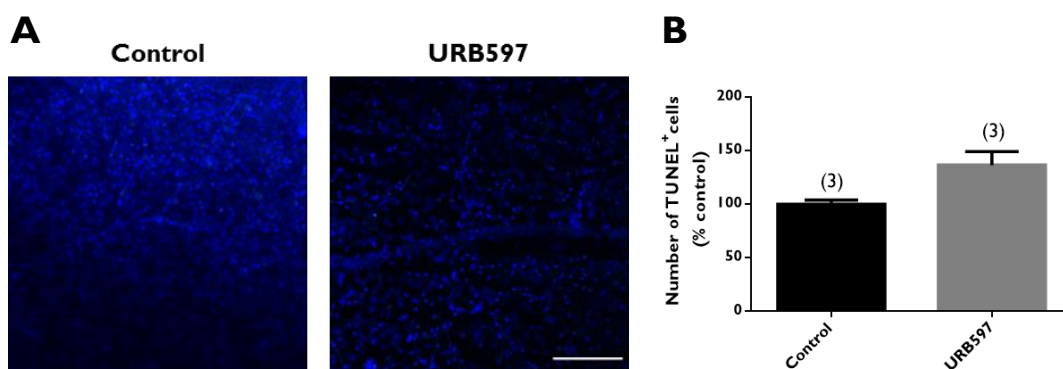


**Figure 25 - Evaluation of the potential of URB597 to induce apoptotic cell death in retinal explants.** Retinal explants were cultured for 3 days and challenged with  $10 \mu\text{M}$  URB597 (FAAH inhibitor), at day 2 in culture. **(A)** Apoptotic cell death was assessed with TUNEL assay in RGC layer. Nuclei were counterstained with DAPI (blue) and representative images are depicted. Scale Bar:  $50 \mu\text{m}$ . **(B)** Quantification of TUNEL positive cells in RGC layer per field. The results are expressed in percentage of control as mean  $\pm$  SEM. The number of independent experiments is indicated above the bars.

#### 4.6. Effect of elevated hydrostatic pressure (EHP) in RGC survival

The RGC survival was assessed by immunohistochemistry with an antibody that recognizes the transcription factor Brn3a, which is expressed only in RGCs in the retina and can be used to identify these cells (Nadal-Nicolas *et al.*, 2009) (Fig. 26A).

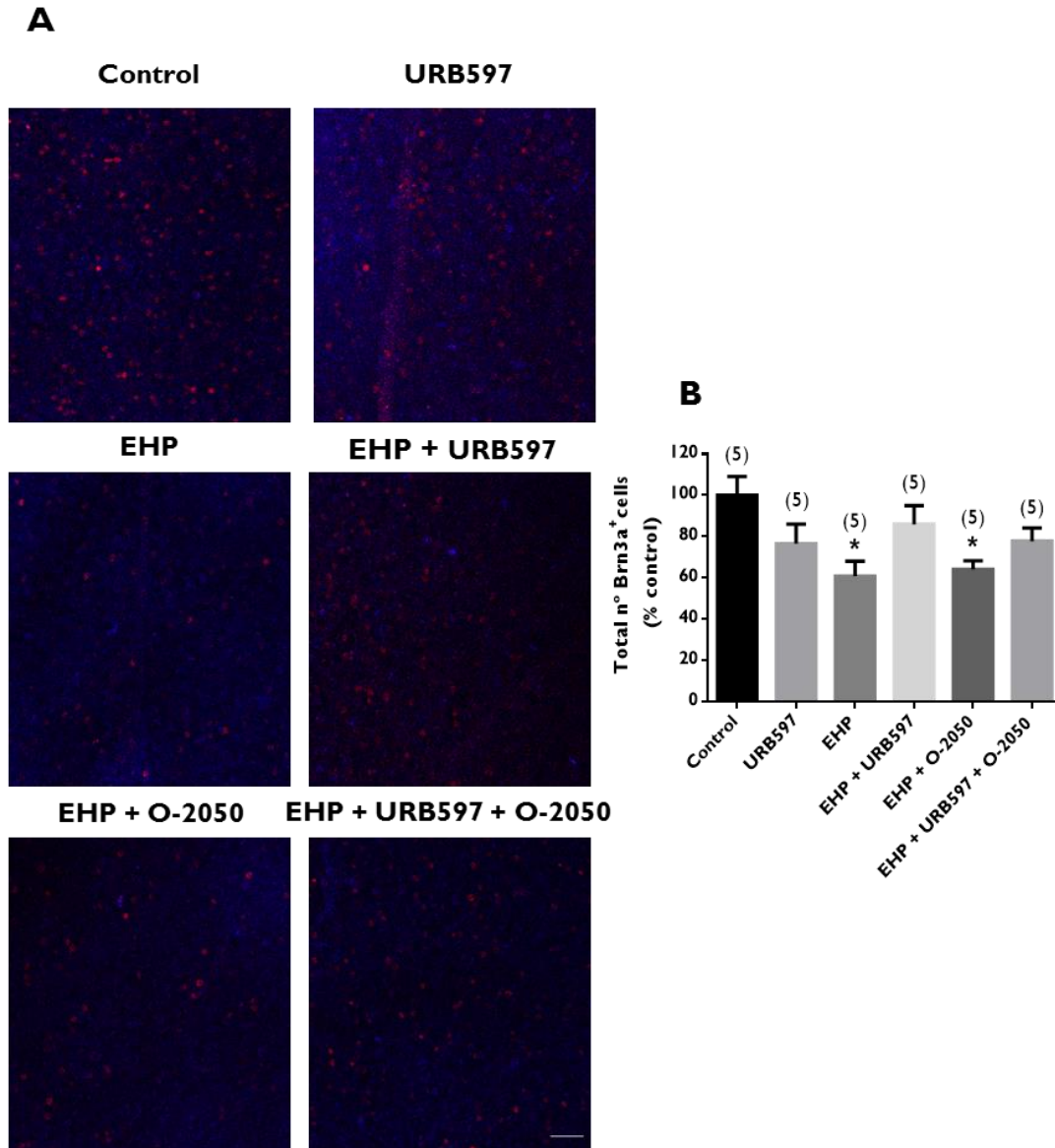


**Figure 26 - Evaluation of the potential protective effect of the FAAH inhibitor, URB597, on RGC survival in retinal explants exposed to EHP.** Retinal explants were cultured for 3 days and challenged with EHP, at day 2 in culture, for 24 h, in the absence or presence of 10  $\mu$ M URB597 (FAAH inhibitor) and/or in the absence or presence of 10  $\mu$ M O-2050 (CB<sub>1</sub> receptor antagonist). **(A)** RGCs were identified by immunohistochemistry with an antibody against Brn3a. Nuclei were counterstained with DAPI (blue) and representative images are depicted. Scale Bar: 50  $\mu$ m. **(B)** Quantification of the number of Brn3a-immunoreactive cells per field in each experimental condition indicated below bars. The results are expressed in percentage of control as mean  $\pm$  SEM. The number of independent experiments is indicated above the bars. \* $p < 0.05$ , compared with Control, One-way ANOVA followed by Holm-Sidak's multiple comparisons test.

Recent studies from our group demonstrated that exposure to EHP decreases RGC survival (Madeira *et al.*, 2015b). In fact, in retinal explants challenged with EHP, it was also found there was a significant decrease ( $p < 0.05$ ) in the number of Brn3a<sup>+</sup> cells to  $60.8 \pm 7.3\%$  of control ( $125.8 \pm 11.41$  cells per field) (Fig. 26B). In retinal explants treated with URB597, RGC loss induced by EHP was less pronounced ( $76.57 \pm 9.5\%$  of control), and this decrease in RGCs was not significantly different from control. However, this partial protective effect induced by URB597 did not reach statistical significance comparing to the condition where retinal explants were challenged with EHP. When retinal explants were challenged with EHP, in the presence of CB<sub>1</sub> receptor antagonist, O-2050 (10  $\mu$ M), there was also a decrease in the number of Brn3a<sup>+</sup> cells ( $64.1 \pm 4.2\%$  of control,  $p < 0.05$ ), an effect similar to what was found when retinal explants were challenged with EHP ( $60.8 \pm 7.3\%$  of control). Moreover, the presence of O-2050 did not significantly affect the partial protective effect induced by URB597 against RGC death triggered by EHP, suggesting that the activation of CB<sub>1</sub> receptor apparently did not mediate the partial protective effect of URB597, but this issue needs to be clarified with additional experiments.

#### **4.7. Evaluation of the potential effect of FAAH inhibitor, URB597, in microglial morphology in retinal explants**

Microglial cells present a ramified morphology under physiological conditions, which is associated with a surveillance phenotype. Changes in tissue homeostasis may lead microglia to adopt a less ramified morphology, in agreement with a reactive phenotype (Kettenmann *et al.*, 2011). In our group, it was demonstrated previously that EHP induces alterations in microglial morphology in retinal explants, switching to a more amoeboid-like morphology (Madeira *et al.*, 2015b). Based on this evidence, it was investigated if the FAAH inhibitor, URB597, could modulate microglial reactivity induced by EHP in cultured retinal explants, by assessing morphological alterations after CD11b labelling (Fig. 27A). It was also aimed to evaluate whether the potential effect of URB597 on microglial cell morphology could be mediated by CB<sub>1</sub> receptor activation, incubating retinal explants with an antagonist of CB<sub>1</sub> receptor, O-2050 (10  $\mu$ M). In order to evaluate the changes in microglia morphology, was assessed four different morphological parameters in microglial cells: area, perimeter, circularity, and Feret's diameter.

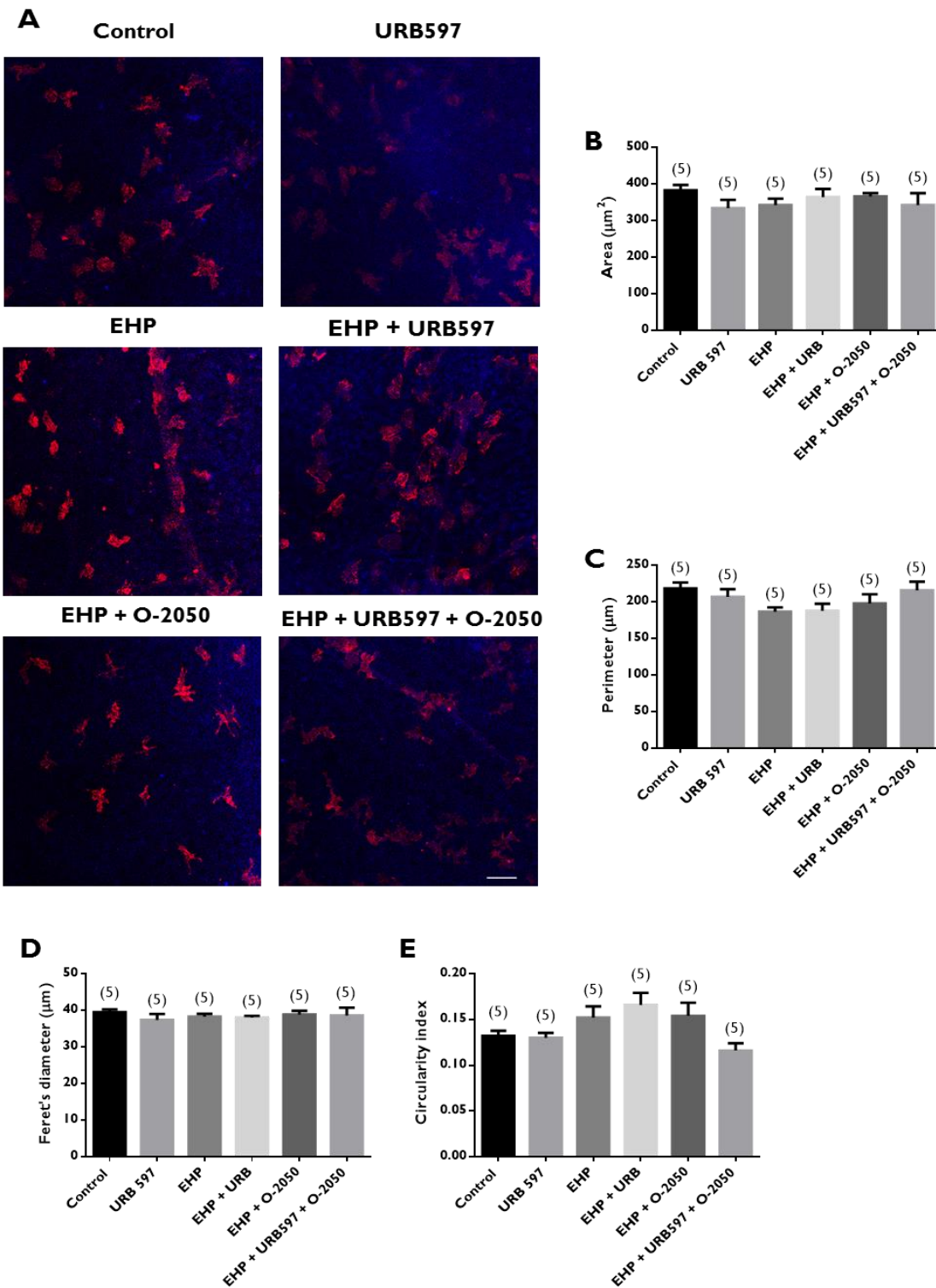


**Figure 27 - Evaluation of the potential effect of FAAH inhibitor, URB597, in microglial morphology in retinal explants.** Retinal explants were cultured for 3 days and challenged with EHP at day 2 in culture, for 24 h, in the absence or presence of 10 µM URB597 (FAAH inhibitor) and/or in the absence or presence of 10 µM O-2050 (CB<sub>1</sub> receptor antagonist). Microglial cells were identified by immunocytochemistry with anti-CD11b. Nuclei were counterstained with DAPI (blue). Representative images are depicted in **A**. Scale Bar: 50 µm. Microglia area (**B**), perimeter (**C**), Feret's diameter (**D**), and circularity index (**E**) were determined using ImageJ. The results are expressed as mean ± SEM. The number of independent experiments is indicated above the bars.

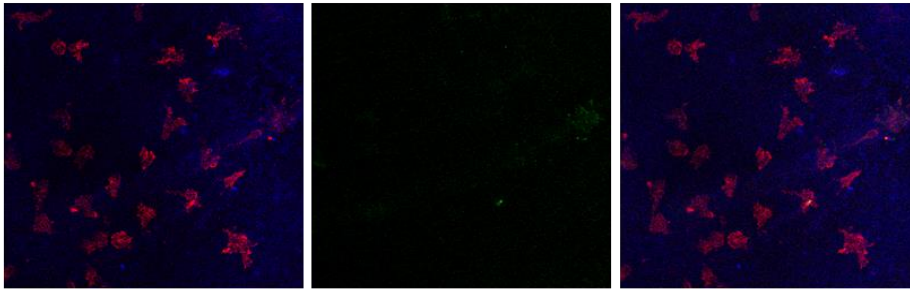
Unexpectedly, we could not observe any significant alterations in microglia morphology triggered by exposure to EHP (Fig. 27). Moreover, we did not detect any significant alteration in microglial cell area (Fig. 27B), perimeter (Fig. 27C), circularity (Fig. 27D), or Feret's diameter (Fig. 27E) between the different conditions tested. These observations contrast with our previous studies, since EHP did not induce microglia morphological alterations.

#### **4.8. Evaluation of the potential effect of FAAH inhibitor, URB597, in microglial iNOS immunoreactivity in retinal explants**

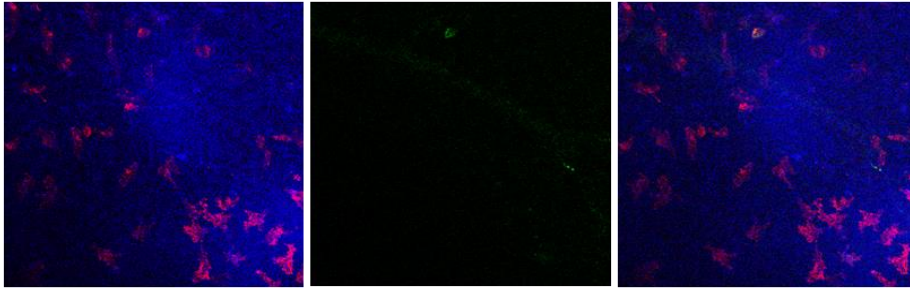
The inducible nitric oxide synthase (iNOS) isoform is one of the enzymes responsible for the synthesis of NO and is typically expressed in response to cellular stress (Morris and Billiar, 1994). It has been shown that NO derived from iNOS plays a key role in causing tissue damage and inflammation. Moreover, iNOS may play essential roles in the degenerative mechanisms in acute glaucoma model (Cho *et al.*, 2011). Taking this into account, it was evaluated iNOS immunoreactivity (iNOS-IR) in microglial cells localized in the RGC layer of retinal explants, after 24 h exposure to EHP. Microglial cells were identified by CD11b immunostaining. In control conditions, iNOS-IR in microglial cells was barely detected (Fig. 28A). In explants exposed to EHP, iNOS-IR significantly increased ( $p < 0.05$ ), comparing to control. Then was evaluated whether FAAH inhibition could rescue the microglia phenotype triggered by EHP. When retinal explants were treated with URB597, the increase in iNOS-IR induced by EHP was completely inhibited ( $p < 0.05$ , comparing with EHP). This observation suggests that the inhibition of FAAH activity was sufficient to prevent the iNOS increase induced by EHP. We assessed if the inhibitory effect caused by FAAH inhibition was mediated by CB<sub>1</sub> receptor activation, by incubating retinal explants with an antagonist of CB<sub>1</sub> receptors, O-2050 (10  $\mu$ M). The incubation with O-2050 did not block the effect of URB597, suggesting that CB<sub>1</sub> receptor was not involved in the inhibitory effect caused by URB597.

**A**

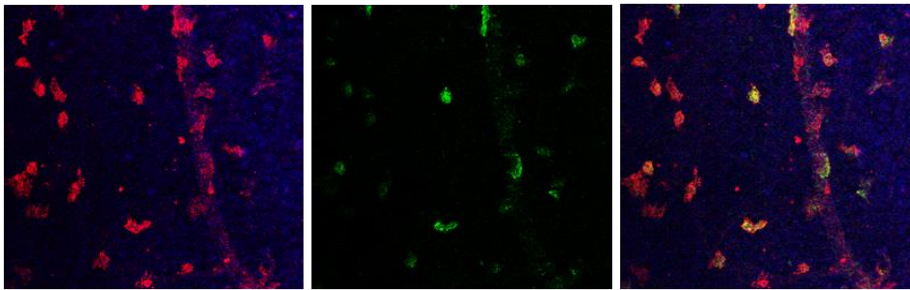
**Control**



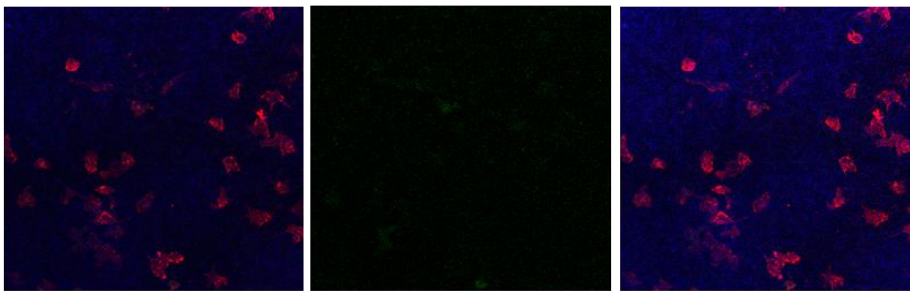
**URB597**



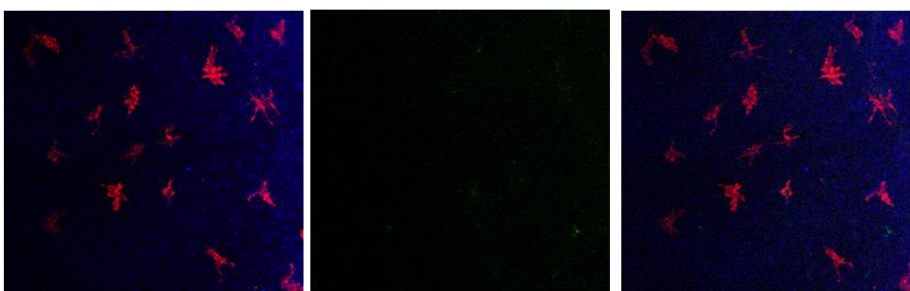
**EHP**



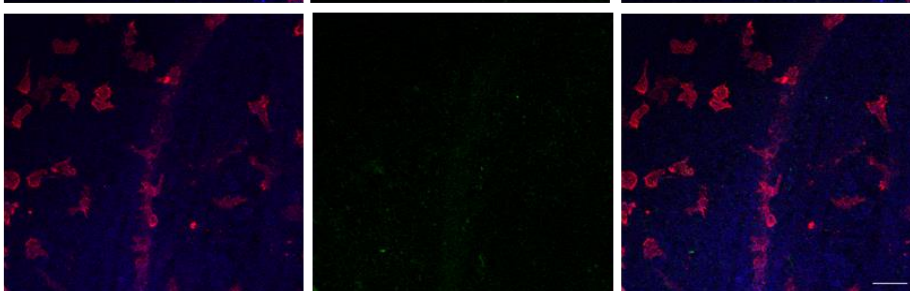
**EHP +  
URB597**



**EHP +  
O-2050**



**EHP +  
URB597 +  
O-2050**



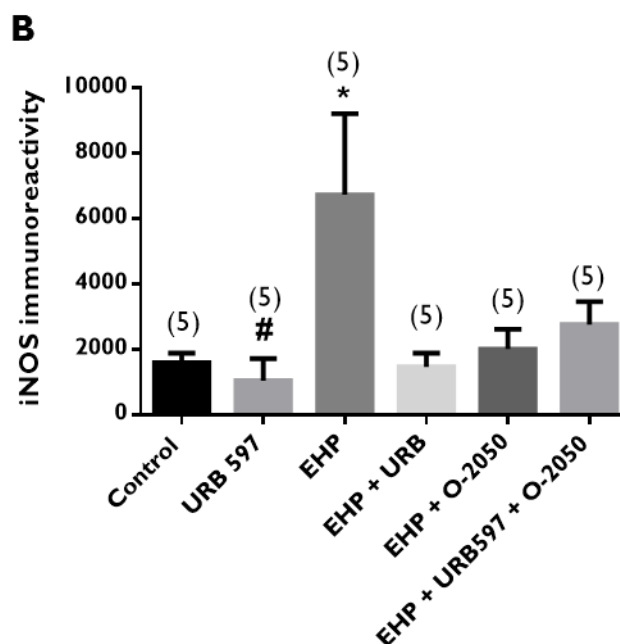


**Figure 28 - Evaluation of the potential effect of FAAH inhibitor, URB597, O-2050, in microglial iNOS-IR in retinal explants.** Retinal explants were cultured for 3 days and challenged with EHP at day 2 in culture, for 24 h, in the absence or presence of 10  $\mu$ M URB597 (FAAH inhibitor) and/or in the absence or presence of 10  $\mu$ M O-2050 (CB<sub>1</sub> receptor antagonist). **(A)** Retinal explants were immunostained for CD11b and for iNOS. Nuclei were stained with DAPI (blue) and representative images are depicted. Scale Bar: 50  $\mu$ m. **(B)** Densitometric analysis for iNOS-IR was determined using ImageJ. The results are expressed as mean  $\pm$  SEM. The number of independent experiments is indicated above the bars. \* $p < 0.05$ , compared with control; # $p < 0.05$ , compared with EHP; One-way ANOVA followed by Holm-Sidak's multiple comparisons test.



# CHAPTER 5

---

*Discussion*



## 5. Discussion

Glaucoma refers to a group of disorders characterized by optic neuropathy with alterations at the ONH, namely excavation of the optic disc, and progressive loss of RGCs. There are several factors that have been associated with the development and progression of glaucoma, such as systemic hypertension, family history, cigarette smoking, among others. However, elevated IOP and age are considered the main risk factors to develop glaucoma (Madeira *et al.*, 2015a; Van de Velde *et al.*, 2015).

There are several animal models of glaucoma, including genetic models (e.g. DBA/2J mice) and inducible models of IOP elevation such as: microbead injections in the anterior chamber (Sappington *et al.*, 2010; Morgan and Tribble, 2015), saline injection in the episcleral veins (Morrison *et al.*, 1997), and EVC (Shareef *et al.*, 1995; Urcola *et al.*, 2006). Regarding the EVC model, it has been described that the sustained increase in IOP leads to RGC death and triggers an inflammatory response including microglial activation (Roh *et al.*, 2012) (Hernandez *et al.*, 2009). This model has proven to be a good model to evaluate drug effects on IOP (Urcola *et al.*, 2006). Therefore, we chose this model and induced a sustained increase in IOP for seven days.

Since elevated IOP is considered the main risk factor of glaucoma, some *in vitro* models have been developed, such as the EHP model, to try to unveil the mechanisms behind glaucomatous disease. In previous studies in our group, exposure to EHP induced neuronal cell apoptosis, namely in RGCs, and glial cell activation (Madeira *et al.*, 2015b).

Pharmacological studies have shown the involvement of ocular CB<sub>1</sub> receptors in the IOP reduction induced by cannabinoids (Tomida *et al.*, 2004). Moreover, the anatomical distribution of cannabinoid receptors suggests a possible influence of endocannabinoids on trabecular and uveoscleral aqueous humour outflow and on aqueous humour production, thus affecting IOP (Tomida *et al.*, 2004). In addition, in a model of ocular hypertension, the topical administration of WIN-55,212-2, a synthetic agonist of CB<sub>1</sub> receptor, in the eye, decreased significantly the IOP which remained low during treatment (Hosseini *et al.*, 2006; Nucci *et al.*, 2008).

The hydrolysis of endocannabinoids, such as AEA, 2-AG, OEA and PEA occurs mainly via FAAH. Thus, by inhibiting FAAH, the levels of endocannabinoids increase in the organism, which may influence IOP. URB597 is a selective FAAH inhibitor and

its effects do not seem to ever been investigated in the context of a model of glaucoma characterized by chronic hypertension. There are only two studies evaluating the effect of URB597 in animal models of retinal degeneration, namely an optic nerve axotomy model (Slusar *et al.*, 2013) and an ischemia-reperfusion injury model (Nucci *et al.*, 2007), showing neuroprotective and anti-inflammatory properties of URB597. Those two models are not chronic glaucoma models since there is not a sustained elevation of IOP. In our EVC model, URB597 significantly decreased IOP in animals with ocular hypertension. We aimed to understand which mechanism mediates the effect of URB597 on IOP, by evaluating the involvement of CB<sub>1</sub> receptors. For this propose, it was administered a CB<sub>1</sub> receptor antagonist, O-2050, in animals with ocular hypertension and treated with URB597. The administration of O-2050 partially inhibited the effect of URB597 on IOP, indicating the involvement of CB<sub>1</sub> receptor activation. A few studies corroborated our results. For instance, pre-treatment with CB<sub>1</sub> receptor antagonists prevented the IOP-lowering effects normally observed after the administration of the metabolically stable analogue of AEA, methanandamide (Pate *et al.*, 1997), or with synthetic cannabinoids such as CP55,940 (Pate *et al.*, 1998) and WIN-55,212-2 (Hosseini *et al.*, 2006;Nucci *et al.*, 2008).

In order to prove that URB597 inhibits FAAH activity in ocular tissues, was measured the FAAH activity in cultured retinal explants under normal hydrostatic pressure conditions or submitted to EHP. As expected, our results show that URB597 significantly inhibited FAAH activity in retinal explants exposed to normal pressure or EHP. In order to understand whether exposure to EHP could affect the levels of endocannabinoids, as well as whether the inhibition of FAAH could trigger an increase in the levels of endocannabinoids in the retina, we evaluated the levels of endocannabinoids (AEA, OEA, and PEA) in retinal explants exposed, or not, to EHP, and treated with URB597. Exposure of retinal explants to EHP for 24 h did not significantly affect the levels of endocannabinoids, at least for this period of exposure to EHP. However, it can be noticed that there was a tendency for an increase in all measured endocannabinoids (AEA, OEA, and PEA). This observation suggests that the retinal tissue appears to slightly respond to this stress condition by increasing endocannabinoids levels. It is likely that for another period of exposure to EHP, it was could detect significant differences. Incubation with URB597 increased AEA, OEA, and PEA levels, both in retinal explants exposed to normal pressure and exposed to EHP. Moreover, in retinal explants exposed to EHP treated with URB597,

the levels of endocannabinoids were even higher, comparing to explants exposed to EHP, thus suggesting that EHP indeed potentiates the accumulation of endocannabinoids in the retina. This is the first time that is shown that EHP can potentiate the accumulation of endocannabinoids in the retinal tissue. Similarly, Fegley and colleagues also showed that FAAH inhibition by URB597 elevates brain AEA and OEA levels and amplifies the pharmacological actions of these endocannabinoids by selectively targeting FAAH activity (Fegley *et al.*, 2005).

As previously mentioned, RGC death is a hallmark of glaucoma, in which several mechanisms might be involved. IOP is considered the main direct inducer of RGC stress and apoptosis. Recent studies in our lab described that exposure to EHP decreases RGC survival in retinal explants (Madeira *et al.*, 2015b). The FAAH inhibitor, URB597, was shown to delay RGC death in an optic nerve injury animal model (Slusar *et al.*, 2013). In addition, URB597 treatment prevented the increase in FAAH activity in the retina and RGC loss triggered by ocular ischemia, suggesting that reduced levels of AEA caused by enhanced FAAH activity might play a role in the RGC loss provoked by ischemia-reperfusion injury (Nucci *et al.*, 2008). Based on these evidences, we hypothesized that URB597 could afford neuroprotection and prevent RGC death in retinal explants challenged with EHP. However, first was evaluated whether URB597 *per se* could induce cell death in RGC layer in retinal explants, and it was found that URB597 did not induce cell death. Then, was evaluated RGC survival in retinal explants exposed to EHP and treated with URB597. As expected, EHP significantly decreased the number of RGCs. Treatment with URB597 induced a small protective effect, because in retinal explants exposed to EHP, in the presence of URB597, the number of RGCs did not significantly differ from control condition. Slusar and colleagues also found that URB597 protects RGCs in animals submitted to optic nerve injury. These authors also showed that the administration of a CB<sub>1</sub> receptor antagonist, AM281, abolished the effect of URB597 (Slusar *et al.*, 2013). Thus, we also investigated if the partial protective effect of URB597 could be mediated by CB<sub>1</sub> receptors. Unexpectedly, our results suggest that the activation of CB<sub>1</sub> receptors did not mediate the protective effect of URB597 on RGC survival. We must emphasize that the model we used in these experiments may correspond to a more severe injury compared to the model used by Slusar and colleagues, since, in addition to RGC axotomy to isolate the retinas, the retinas are exposed to EHP. As a consequence, other receptors might be involved in the protective effect of URB597, which may explain no major contribution of CB<sub>1</sub> receptor. Moreover, we used a

different CB<sub>1</sub> receptor antagonist, O-2050, which is a neutral cannabinoid CB<sub>1</sub> receptor antagonist and has a higher affinity to CB<sub>1</sub> receptor comparing with AM281, which is an antagonist/inverse agonist of CB<sub>1</sub> receptors (Süudhof, 2008). Despite this, we cannot draw a final conclusion about our results. Additional experiments are necessary to increase the number of independent experiments.

Neuroinflammation has been described as an important player in the pathogenesis of glaucoma, by activating glial cells that initiate an inflammatory response (Madeira *et al.*, 2015a). Under glaucomatous conditions, retinal microglial cells present alterations in morphology, gene expression, proliferation and immune response, compatible with a reactive phenotype (Karlstetter *et al.*, 2010; Madeira *et al.*, 2015a). In the resting state, microglia actively survey their microenvironment with extremely motile processes and protrusions, having a ramified morphology (Kettenmann *et al.*, 2011; Li *et al.*, 2015). When a retinal insult occurs, microglial cells localized in RGC layer become activated, changing their morphology and becoming more amoeboid and less ramified (Karlstetter *et al.*, 2010; Saijo and Glass, 2011). In our laboratory, we have demonstrated that EHP induces alterations in microglial morphology, in retinal explants, switching to a more amoeboid-like morphology (Madeira *et al.*, 2015b). Herein, we investigated if URB597 could modulate microglial reactivity induced by EHP in cultured retinal explants, by assessing morphological alterations, using several parameters (area, perimeter, circularity, and Feret's diameter). We also aimed to evaluate whether the potential effect of URB597 could be mediated by CB<sub>1</sub> receptor activation. Unexpectedly, we did not find any evidence of morphological changes in retinal microglia, although in previous experiments these morphological changes were consistent. This unexpected result might be related with slightly different experimental conditions, as in this study retinal explants were 1 day less in culture than in the others studies developed in our laboratory. It has been described that with more days in culture retinal explants present more cell degeneration (Buonfiglio *et al.*, 2014), and this is correlated with an increase in microglia activation. This might explain why we did not observe significant changes in microglia morphology. Nevertheless, there are two studies showing that microglia activation in mice retinal explants increases upon an insult, but without significant changes in cell ramification (Lee *et al.*, 2008; Kettenmann *et al.*, 2011), indicating that using microglia morphology as a single parameter to measure microglia activation is restrictive.

The inducible isoform of NOS (iNOS) is one of the enzymes responsible for the production of NO and is typically expressed in response to cellular stress (Morris

and Billiar, 1994). It has been shown that NO derived from iNOS plays a key role in an acute glaucoma model, causing inflammation and tissue damage (Cho *et al.*, 2011). Moreover, the activation of microglial cells leads to the production of pro-inflammatory and cytotoxic factors like NO, both *in vivo* and *in vitro* (Kraft and Harry, 2011). *In vitro* studies developed in our laboratory have shown that exposure to EHP significantly increases iNOS immunoreactivity (iNOS-IR), mainly in microglial cells, confirming that these cells are the main producers of NO under these conditions (Madeira *et al.*, 2015b). Therefore, in this study, to evaluate retinal microglia reactivity we analysed iNOS-IR in microglial cells in retinal explants exposed to EHP. As expected, EHP increased iNOS-IR in retinal microglia localized in RGC layer. We then evaluated whether treatment with URB597 could inhibit the upregulation of iNOS in microglial cells. In fact, the inhibition of FAAH activity was sufficient to block the iNOS increase induced by EHP, indicating that endocannabinoids control microglia reactivity. However, the results failed to demonstrate that CB<sub>1</sub> receptors activation was mediating the inhibitory effect of URB597, downregulating iNOS-IR. On the contrary, the application of O-2050 in retinal explants exposed to EHP appears to prevent the increase in iNOS-IR triggered by EHP, suggesting that CB<sub>1</sub> receptor activation, and not CB<sub>1</sub> receptor inhibition, could be partly involved in the increase of iNOS-IR in microglial cells, as previously shown (Waksman *et al.*, 1999; Cabral *et al.*, 2001). Thus, other receptors or mechanisms might be responsible for the effect URB597, this however needs to be clarified because our results are not conclusive and more experiments are needed.

In summary, our results indicate that the selective FAAH inhibitor, URB597, decreases IOP in an animal model of ocular hypertension and this effect seems to be partially mediated by CB<sub>1</sub> receptor activation. In *in vitro* studies, we also demonstrated that URB597 increases the levels of endocannabinoids (AEA, OEA, and PEA) in the retina, and inhibits the degeneration of RGCs and the upregulation of iNOS expression in retinal microglial cells induced by EHP. In some experiments, it appears that CB<sub>1</sub> receptor activation mediates, at least partially, the effects of URB597, but this needs to be confirmed, because the results are not entirely conclusive. Despite this, FAAH enzyme might be considered a potential therapeutic target worth to investigate in the context of glaucoma, once FAAH inhibition has the potential to decrease IOP, control neuroinflammation, and afford neuroprotection to RGCs. Further studies must be performed to better understand the mechanisms by which URB597 is able to exert anti-inflammatory and neuroprotective actions.



# CHAPTER 6

---

*Conclusions*



## 6. Conclusions

According to the results obtained in this thesis, we demonstrated that:

- The selective FAAH inhibitor, URB597, significantly decreases IOP in an animal model of ocular hypertension, and this effect seems to be partially mediated by CB<sub>1</sub> receptor activation;
- In retinal explants submitted to EHP, URB597 inhibits FAAH activity leading to the increase of the levels of endocannabinoids (AEA, OEA, and PEA);
- In retinal explants challenged with EHP, URB597 inhibited RGC loss induced by EHP exposure. The activation of CB<sub>1</sub> receptors does not seem to mediate the protective effect of URB597 on RGC survival;
- URB597 inhibits the upregulation of iNOS immunoreactivity in microglial cells induced by EHP exposure in retinal explants. Again, the CB<sub>1</sub> receptor does not seem to mediate the inhibitory effect of URB597.

In summary, this study clearly shows that FAAH enzyme represents a potential therapeutic target worth to investigate in the context of glaucoma, since FAAH inhibition has the potential to decrease IOP, control neuroinflammation, and afford neuroprotection against RGC degeneration. However, further studies must be performed to better understand the mechanisms by which URB597 is able to exert anti-inflammatory and neuroprotective actions.

### Future perspectives

We will increase the number of independent experiments already performed in retinal explants exposed to EHP to clarify the effect of URB597 and CB<sub>1</sub> receptors on retinal neuroinflammation and RGC protection. Moreover, it would be interesting to evaluate the expression and release of pro-inflammatory cytokines in retinal explants exposed to the same experimental conditions.

It would be also interesting to extend the duration of the ocular hypertension model (EVC) up to 14 days, in order to assess the anti-inflammatory and neuroprotective potential of URB597 treatment.

In addition, to better understand the modulation of the endocannabinoid system, we would like to evaluate the involvement of the CB<sub>2</sub> receptors in the effects induced by URB597 treatment in both models, animals with ocular hypertension and retinal explants exposed to EHP.



# CHAPTER 7

---

*References*



## 7. References

- AGAR, A.; LI, S.; AGARWAL, N.; CORONEO, M. T.; HILL, M. A. (2006) - Retinal ganglion cell line apoptosis induced by hydrostatic pressure. "Brain Res". 1086 (2006) 1 191-200.
- AGAR, A.; YIP, S. S.; HILL, M. A.; CORONEO, M. T. (2000) - Pressure related apoptosis in neuronal cell lines. "J Neurosci Res". 60 (2000) 4 495-503.
- ALMASIEH, M.; WILSON, A. M.; MORQUETTE, B.; CUEVA VARGAS, J. L.; DI POLO, A. (2012) - The molecular basis of retinal ganglion cell death in glaucoma. "Prog Retin Eye Res". 31 (2012) 2 152-81.
- BAI, Y.; ZHU, Y.; CHEN, Q.; XU, J.; SARUNIC, M. V.; SARAGOVI, U. H.; ZHUO, Y. (2014) - Validation of glaucoma-like features in the rat episcleral vein cauterization model. "Chin Med J (Engl)". 127 (2014) 2 359-64.
- BALTMER, A.; DUGGAN, J.; NIZARI, S.; SALT, T. E.; CORDEIRO, M. F. (2010) - Neuroprotection in glaucoma - Is there a future role? "Exp Eye Res". 91 (2010) 5 554-66.
- BAUR, R.; GERTSCH, J.; SIGEL, E. (2013) - Do N-arachidonyl-glycine (NA-glycine) and 2-arachidonoyl glycerol (2-AG) share mode of action and the binding site on the beta2 subunit of GABAA receptors? "PeerJ". 1 (2013) e149.
- BOSCO, A.; STEELE, M. R.; VETTER, M. L. (2011) - Early microglia activation in a mouse model of chronic glaucoma. "J Comp Neurol". 519 (2011) 4 599-620.
- BOUSKILA, J.; BURKE, M. W.; ZABOURI, N.; CASANOVA, C.; PTITO, M.; BOUCHARD, J. F. (2012) - Expression and localization of the cannabinoid receptor type 1 and the enzyme fatty acid amide hydrolase in the retina of vervet monkeys. "Neuroscience". 202 (2012) 1 17-30.
- BUONFIGLIO, D. C.; MALAN, A.; SANDU, C.; JAEGER, C.; CIPOLLA-NETO, J.; HICKS, D.; FELDER-SCHMITTBUHL, M. P. (2014) - Rat retina shows robust circadian expression of clock and clock output genes in explant culture. "Mol Vis". 20 (2014) 742-52.
- CABRAL, G. A.; HARMON, K. N.; CARLISLE, S. J. (2001) - Cannabinoid-mediated inhibition of inducible nitric oxide production by rat microglial cells: evidence for CB1 receptor participation. "Adv Exp Med Biol". 493 (2001) 207-14.
- CHANG, E. E.; GOLDBERG, J. L. (2012) - Glaucoma 2.0: neuroprotection, neuroregeneration, neuroenhancement. "Ophthalmology". 119 (2012) 5 979-86.
- CHEN, Y. S.; GREEN, C. R.; DANESH-MEYER, H. V.; RUPENTHAL, I. D. (2015) - Neuroprotection in the treatment of glaucoma - A focus on connexin43 gap junction channel blockers. "Eur J Pharm Biopharm". (2015)
- CHO, K. J.; KIM, J. H.; PARK, H. Y.; PARK, C. K. (2011) - Glial cell response and iNOS expression in the optic nerve head and retina of the rat following acute high IOP ischemia-reperfusion. "Brain Res". 1403 (2011) 67-77.

## References

- CHONG, R. S.; MARTIN, K. R. (2015) - Glial cell interactions and glaucoma. "Curr Opin Ophthalmol". 26 (2015) 2 73-7.
- CUNHA-VAZ, J.; BERNARDES, R.; LOBO, C. (2011) - Blood-retinal barrier. "Eur J Ophthalmol". 21 Suppl 6 (2011) S3-9.
- DANIAS, J.; SHEN, F.; KAVALARAKIS, M.; CHEN, B.; GOLDBLUM, D.; LEE, K.; ZAMORA, M. F.; SU, Y.; BRODIE, S. E.; PODOS, S. M.; MITTAG, T. (2006) - Characterization of retinal damage in the episcleral vein cauterization rat glaucoma model. "Exp Eye Res". 82 (2006) 2 219-28.
- DI MARZO, V.; BIFULCO, M.; DE PETROCELLIS, L. (2004) - The endocannabinoid system and its therapeutic exploitation. "Nat Rev Drug Discov". 3 (2004) 9 771-84.
- DI MARZO, V.; DE PETROCELLIS, L.; BISOGNO, T. (2005) - The biosynthesis, fate and pharmacological properties of endocannabinoids. "Handb Exp Pharmacol". (2005) 168 147-85.
- DOUCETTE, L. P.; RASNITSYN, A.; SEIFI, M.; WALTER, M. A. (2015) - The interactions of genes, age, and environment in glaucoma pathogenesis. "Surv Ophthalmol". 60 (2015) 4 310-326.
- ELJASCHEWITSCH, E.; WITTING, A.; MAWRIN, C.; LEE, T.; SCHMIDT, P. M.; WOLF, S.; HOERTNAGL, H.; RAINE, C. S.; SCHNEIDER-STOCK, R.; NITSCH, R.; ULLRICH, O. (2006) - The endocannabinoid anandamide protects neurons during CNS inflammation by induction of MKP-1 in microglial cells. "Neuron". 49 (2006) 1 67-79.
- FEGLEY, D.; GAETANI, S.; DURANTI, A.; TONTINI, A.; MOR, M.; TARZIA, G.; PIOMELLI, D. (2005) - Characterization of the fatty acid amide hydrolase inhibitor cyclohexyl carbamic acid 3'-carbamoyl-biphenyl-3-yl ester (URB597): effects on anandamide and oleoylethanolamide deactivation. "J Pharmacol Exp Ther". 313 (2005) 1 352-8.
- FERNANDES, K. A.; HARDER, J. M.; WILLIAMS, P. A.; RAUSCH, R. L.; KIERNAN, A. E.; NAIR, K. S.; ANDERSON, M. G.; JOHN, S. W.; HOWELL, G. R.; LIBBY, R. T. (2015) - Using genetic mouse models to gain insight into glaucoma: Past results and future possibilities. "Exp Eye Res". (2015)
- GAVET, O.; PINES, J. (2010) - Progressive activation of CyclinB1-Cdk1 coordinates entry to mitosis. "Dev Cell". 18 (2010) 4 533-43.
- GELATT, K. N.; MACKAY, E. O. (1998) - Distribution of intraocular pressure in dogs. "Vet Ophthalmol". 1 (1998) 2-3 109-114.
- HARRY, G. J. (2013) - Microglia during development and aging. "Pharmacol Ther". 139 (2013) 3 313-26.
- HERNANDEZ, M.; PEARCE-KELLING, S. E.; RODRIGUEZ, F. D.; AGUIRRE, G. D.; VECINO, E. (2010) - Altered expression of retinal molecular markers in the canine RPE65 model of Leber congenital amaurosis. "Invest Ophthalmol Vis Sci". 51 (2010) 12 6793-802.
- HERNANDEZ, M.; RODRIGUEZ, F. D.; SHARMA, S.; VECINO, E. (2009) - Immunohistochemical

- changes in rat retinas at various time periods of elevated intraocular pressure. "Mol Vis". 15 (2009) 2696-709.
- HERNANGÓMEZ, M.; CARRILLO-SALINAS, F. J.; MECHA, M.; CORREA, F.; MESTRE, L.; LORÍA, F.; FELIÚ, A.; DOCAGNE, F.; GUAZA, C. (2014) - Brain Innate Immunity in the Regulation of Neuroinflammation: Therapeutic Strategies by Modulating CD200-CD200R Interaction Involve the Cannabinoid System. "Curr Pharm Des". 20 (2014) 29 4707-22.
- HOSOYA, K., AND TOMI, M.- - **Inner Blood—Retinal Barrier: Transport Biology and Methodology**. In: Drug Absorption Studies. 2008.
- HOSSEINI, A.; LATTANZIO, F. A.; WILLIAMS, P. B.; TIBBS, D.; SAMUDRE, S. S.; ALLEN, R. C. (2006) - Chronic topical administration of WIN-55-212-2 maintains a reduction in IOP in a rat glaucoma model without adverse effects. "Exp Eye Res". 82 (2006) 5 753-9.
- HU, S. S.; ARNOLD, A.; HUTCHENS, J. M.; RADICKE, J.; CRAVATT, B. F.; WAGER-MILLER, J.; MACKIE, K.; STRAIKER, A. (2010) - Architecture of cannabinoid signaling in mouse retina. "J Comp Neurol". 518 (2010) 18 3848-66.
- ISHIKAWA, M.; YOSHITOMI, T.; ZORUMSKI, C. F.; IZUMI, Y. (2010) - Effects of acutely elevated hydrostatic pressure in a rat ex vivo retinal preparation. "Invest Ophthalmol Vis Sci". 51 (2010) 12 6414-23.
- ISHIKAWA, M.; YOSHITOMI, T.; ZORUMSKI, C. F.; IZUMI, Y. (2011) - Downregulation of glutamine synthetase via GLAST suppression induces retinal axonal swelling in a rat ex vivo hydrostatic pressure model. "Invest Ophthalmol Vis Sci". 52 (2011) 9 6604-16.
- JAYAMANNE, A.; GREENWOOD, R.; MITCHELL, V. A.; ASLAN, S.; PIOMELLI, D.; VAUGHAN, C. W. (2006) - Actions of the FAAH inhibitor URB597 in neuropathic and inflammatory chronic pain models. "Br J Pharmacol". 147 (2006) 3 281-8.
- JOOSTEN, M. M.; BALVERS, M. G.; VERHOECKX, K. C.; HENDRIKS, H. F.; WITKAMP, R. F. (2010) - Plasma anandamide and other N-acyl ethanolamines are correlated with their corresponding free fatty acid levels under both fasting and non-fasting conditions in women. "Nutr Metab (Lond)". 7 (2010) 49.
- KANEDA, M. (2013) - Signal processing in the mammalian retina. "J Nippon Med Sch". 80 (2013) 1 16-24.
- KARLSTETTER, M.; EBERT, S.; LANGMANN, T. (2010) - Microglia in the healthy and degenerating retina: insights from novel mouse models. "Immunobiology". 215 (2010) 9-10 685-91.
- KETTENMANN, H.; HANISCH, U. K.; NODA, M.; VERKHRATSKY, A. (2011) - Physiology of microglia. "Physiol Rev". 91 (2011) 2 461-553.
- KIERDORF, K.; PRINZ, M. (2013) - Factors regulating microglia activation. "Front Cell Neurosci". 7 (2013) 44.
- KLAASSEN, I.; VAN NOORDEN, C. J.; SCHLINGEMANN, R. O. (2013) - Molecular basis of the inner blood-retinal barrier and its breakdown in diabetic macular edema and other

## References

- pathological conditions. "Prog Retin Eye Res". 34 (2013) 19-48.
- KOLB, H.- **Simple Anatomy of the Retina**. In: Webvision: The Organization of the Retina and Visual System. Salt Lake City (UT): University of Utah Health Sciences Center, 1995.
- KRAFT, A. D.; HARRY, G. J. (2011) - Features of Microglia and Neuroinflammation Relevant to Environmental Exposure and Neurotoxicity. "Int J Environ Res Public Health". 8 (2011) 7 2980-3018.
- KURPIUS, D.; WILSON, N.; FULLER, L.; HOFFMAN, A.; DAILEY, M. E. (2006) - Early activation, motility, and homing of neonatal microglia to injured neurons does not require protein synthesis. "Glia". 54 (2006) 1 58-70.
- LANGMANN, T. (2007) - Microglia activation in retinal degeneration. "J Leukoc Biol". 81 (2007) 6 1345-51.
- LEE, J. E.; LIANG, K. J.; FARISS, R. N.; WONG, W. T. (2008) - Ex vivo dynamic imaging of retinal microglia using time-lapse confocal microscopy. "Invest Ophthalmol Vis Sci". 49 (2008) 9 4169-76.
- LI, L.; ETER, N.; HEIDUSCHKA, P. (2015) - The microglia in healthy and diseased retina. "Exp Eye Res". 136 (2015) 116-130.
- MADEIRA, M. H.; BOIA, R.; SANTOS, P. F.; AMBROSIO, A. F.; SANTIAGO, A. R. (2015a) - Contribution of microglia-mediated neuroinflammation to retinal degenerative diseases. "Mediators Inflamm". 2015 (2015a) 673090.
- MADEIRA, M. H.; ELVAS, F.; BOIA, R.; GONÇALVES, F. Q.; CUNHA, R. A.; AMBRÓSIO AÓ, F.; SANTIAGO, A. R. (2015b) - Adenosine A(2A)R blockade prevents neuroinflammation-induced death of retinal ganglion cells caused by elevated pressure. "J Neuroinflammation". 12 (2015b)
- MATSUDA, S.; KANEMITSU, N.; NAKAMURA, A.; MIMURA, Y.; UEDA, N.; KURAHASHI, Y.; YAMAMOTO, S. (1997) - Metabolism of anandamide, an endogenous cannabinoid receptor ligand, in porcine ocular tissues. "Exp Eye Res". 64 (1997) 5 707-11.
- MILENI, M.; KAMTEKAR, S.; WOOD, D. C.; BENSON, T. E.; CRAVATT, B. F.; STEVENS, R. C. (2010) - Crystal structure of fatty acid amide hydrolase bound to the carbamate inhibitor URB597: discovery of a deacylating water molecule and insight into enzyme inactivation. "J Mol Biol". 400 (2010) 4 743-54.
- MIYAZAKI, Y.; MATSUO, T.; KURABAYASHI, Y. (2000) - Immobilization stress induces elevation of intraocular pressure in rabbits. "Ophthalmic Res". 32 (2000) 6 270-7.
- MOR, M.; RIVARA, S.; LODOLA, A.; PLAZZI, P. V.; TARZIA, G.; DURANTI, A.; TONTINI, A.; PIERSANTI, G.; KATHURIA, S.; PIOMELLI, D. (2004) - Cyclohexylcarbamic acid 3'- or 4'-substituted biphenyl-3-yl esters as fatty acid amide hydrolase inhibitors: synthesis, quantitative structure-activity relationships, and molecular modeling studies. "J Med Chem". 47 (2004) 21 4998-5008.

- MORGAN, J. E.; TRIBBLE, J. R. (2015) - Microbead models in glaucoma. "Exp Eye Res". (2015)
- MORRIS, S. M., JR.; BILLIAR, T. R. (1994) - New insights into the regulation of inducible nitric oxide synthesis. "Am J Physiol". 266 (1994) 6 Pt 1 E829-39.
- MORRISON, J. C.; JIA, L.; CEPURNA, W.; GUO, Y.; JOHNSON, E. (2009) - Reliability and sensitivity of the TonoLab rebound tonometer in awake Brown Norway rats. "Invest Ophthalmol Vis Sci". 50 (2009) 6 2802-8.
- MORRISON, J. C.; MOORE, C. G.; DEPPMEIER, L. M.; GOLD, B. G.; MESHUL, C. K.; JOHNSON, E. C. (1997) - A rat model of chronic pressure-induced optic nerve damage. "Exp Eye Res". 64 (1997) 1 85-96.
- MURPHY, D. F. (1985) - Anesthesia and intraocular pressure. "Anesth Analg". 64 (1985) 5 520-30.
- NADAL-NICOLAS, F. M.; JIMENEZ-LOPEZ, M.; SOBRADO-CALVO, P.; NIETO-LOPEZ, L.; CANOVAS-MARTINEZ, I.; SALINAS-NAVARRO, M.; VIDAL-SANZ, M.; AGUDO, M. (2009) - Brn3a as a marker of retinal ganglion cells: qualitative and quantitative time course studies in naive and optic nerve-injured retinas. "Invest Ophthalmol Vis Sci". 50 (2009) 8 3860-8.
- NUCCI, C.; BARI, M.; SPANO, A.; CORASANITI, M.; BAGETTA, G.; MACCARRONE, M.; MORRONE, L. A. (2008) - Potential roles of (endo)cannabinoids in the treatment of glaucoma: from intraocular pressure control to neuroprotection. "Prog Brain Res". 173 (2008) 451-64.
- NUCCI, C.; GASPERI, V.; TARTAGLIONE, R.; CERULLI, A.; TERRINONI, A.; BARI, M.; DE SIMONE, C.; AGRO, A. F.; MORRONE, L. A.; CORASANITI, M. T.; BAGETTA, G.; MACCARRONE, M. (2007) - Involvement of the endocannabinoid system in retinal damage after high intraocular pressure-induced ischemia in rats. "Invest Ophthalmol Vis Sci". 48 (2007) 7 2997-3004.
- OVERBY, D. R.; CLARK, A. F. (2015) - Animal models of glucocorticoid-induced glaucoma. "Exp Eye Res". (2015)
- PACHER, P.; BATKAI, S.; KUNOS, G. (2006) - The endocannabinoid system as an emerging target of pharmacotherapy. "Pharmacol Rev". 58 (2006) 3 389-462.
- PATE, D. W.; JARVINEN, K.; URTTI, A.; JARHO, P.; MAHADEVAN, V.; JARVINEN, T. (1997) - Effects of topical alpha-substituted anandamides on intraocular pressure in normotensive rabbits. "Pharm Res". 14 (1997) 12 1738-43.
- PATE, D. W.; JARVINEN, K.; URTTI, A.; MAHADEVAN, V.; JARVINEN, T. (1998) - Effect of the CBI receptor antagonist, SR141716A, on cannabinoid-induced ocular hypotension in normotensive rabbits. "Life Sci". 63 (1998) 24 2181-8.
- PERTWEE, R. G. (1997) - Pharmacology of cannabinoid CBI and CB2 receptors. "Pharmacol Ther". 74 (1997) 2 129-80.
- PERTWEE, R. G. (2005) - Pharmacological actions of cannabinoids. "Handb Exp Pharmacol".

## References

- (2005) 168 1-51.
- PERTWEE, R. G. - **Cannabinoids**. Springer, 2006. ISBN 9783540265733
- PURVES, D. - **Neuroscience**. Third edition edn. Sunderland, Massachusetts U.S.A.: Sinauer Associates, Inc., 2004.
- QU, J.; WANG, D.; GROSSKREUTZ, C. L. (2010) - Mechanisms of retinal ganglion cell injury and defense in glaucoma. "Exp Eye Res". 91 (2010) 1 48-53.
- REICHENBACH, A.; BRINGMANN, A. (2013) - New functions of Muller cells. "Glia". 61 (2013) 5 651-78.
- RIVERS, J. R.; ASHTON, J. C. (2010) - The development of cannabinoid CB1 receptor agonists for the treatment of central neuropathies. "Cent Nerv Syst Agents Med Chem". 10 (2010) 1 47-64.
- ROH, M.; ZHANG, Y.; MURAKAMI, Y.; THANOS, A.; LEE, S. C.; VAVVAS, D. G.; BENOWITZ, L. I.; MILLER, J. W. (2012) - Etanercept, a widely used inhibitor of tumor necrosis factor- $\alpha$  (TNF- $\alpha$ ), prevents retinal ganglion cell loss in a rat model of glaucoma. "PLoS One". 7 (2012) 7 e40065.
- SAIJO, K.; GLASS, C. K. (2011) - Microglial cell origin and phenotypes in health and disease. "Nat Rev Immunol". 11 (2011) 11 775-87.
- SANTIAGO, A. R.; BAPTISTA, F. I.; SANTOS, P. F.; CRISTOVAO, G.; AMBROSIO, A. F.; CUNHA, R. A.; GOMES, C. A. (2014) - Role of microglia adenosine A<sub>2A</sub> receptors in retinal and brain neurodegenerative diseases. "Mediators Inflamm". 2014 (2014) 465694.
- SAPPINGTON, R. M.; CARLSON, B. J.; CRISH, S. D.; CALKINS, D. J. (2010) - The microbead occlusion model: a paradigm for induced ocular hypertension in rats and mice. "Invest Ophthalmol Vis Sci". 51 (2010) 1 207-16.
- SAPPINGTON, R. M.; SIDOROVA, T.; LONG, D. J.; CALKINS, D. J. (2009) - TRPV1: contribution to retinal ganglion cell apoptosis and increased intracellular Ca<sup>2+</sup> with exposure to hydrostatic pressure. "Invest Ophthalmol Vis Sci". 50 (2009) 2 717-28.
- SHAREEF, S. R.; GARCIA-VALENZUELA, E.; SALIERNO, A.; WALSH, J.; SHARMA, S. C. (1995) - Chronic ocular hypertension following episcleral venous occlusion in rats. "Exp Eye Res". 61 (1995) 3 379-82.
- SLUSAR, J. E.; CAIRNS, E. A.; SZCZESNIAK, A. M.; BRADSHAW, H. B.; DI POLO, A.; KELLY, M. E. (2013) - The fatty acid amide hydrolase inhibitor, URB597, promotes retinal ganglion cell neuroprotection in a rat model of optic nerve axotomy. "Neuropharmacology". 72 (2013) 1 16-25.
- STRAIKER, A. J.; MAGUIRE, G.; MACKIE, K.; LINDSEY, J. (1999) - Localization of cannabinoid CB1 receptors in the human anterior eye and retina. "Invest Ophthalmol Vis Sci". 40 (1999) 10 2442-8.
- SÜUDHOF, T. C. - **Neurotransmitter release**. Springer, 2008. ISBN 3540748040
- TEZEL, G. (2011) - The immune response in glaucoma: a perspective on the roles of oxidative

- stress. "Exp Eye Res". 93 (2011) 2 178-86.
- THAM, C. S.; WHITAKER, J.; LUO, L.; WEBB, M. (2007) - Inhibition of microglial fatty acid amide hydrolase modulates LPS stimulated release of inflammatory mediators. "FEBS Lett". 581 (2007) 16 2899-904.
- TO, C. H.; KONG, C. W.; CHAN, C. Y.; SHAHIDULLAH, M.; DO, C. W. (2002) - The mechanism of aqueous humour formation. "Clin Exp Optom". 85 (2002) 6 335-49.
- TOK, L.; NAZIROGLU, M.; UGUZ, A. C.; TOK, O. (2014) - Elevated hydrostatic pressures induce apoptosis and oxidative stress through mitochondrial membrane depolarization in PC12 neuronal cells: A cell culture model of glaucoma. "J Recept Signal Transduct Res". 34 (2014) 5 410-6.
- TOMIDA, I.; PERTWEE, R. G.; AZUARA-BLANCO, A. (2004) - Cannabinoids and glaucoma. "Br J Ophthalmol". 88 (2004) 5 708-13.
- UEDA, N.; TSUBOI, K.; UYAMA, T. (2013) - Metabolism of endocannabinoids and related N-acylethanolamines: canonical and alternative pathways. "Febs j". 280 (2013) 9 1874-94.
- URCOLA, J. H.; HERNANDEZ, M.; VECINO, E. (2006) - Three experimental glaucoma models in rats: comparison of the effects of intraocular pressure elevation on retinal ganglion cell size and death. "Exp Eye Res". 83 (2006) 2 429-37.
- VAN DE VELDE, S.; DE GROEF, L.; STALMANS, I.; MOONS, L.; VAN HOVE, I. (2015) - Towards axonal regeneration and neuroprotection in glaucoma: Rho kinase inhibitors as promising therapeutics. "Prog Neurobiol". (2015)
- VAUGHAN, C. W.; CHRISTIE, M. J. (2005) - Retrograde signalling by endocannabinoids. "Handb Exp Pharmacol". (2005) 168 367-83.
- VECINO, E.; RODRIGUEZ, F. D.; RUZAFI, N.; PEREIRO, X.; SHARMA, S. C. (2015) - Glia-neuron interactions in the mammalian retina. "Prog Retin Eye Res". (2015)
- WAKSMAN, Y.; OLSON, J. M.; CARLISLE, S. J.; CABRAL, G. A. (1999) - The central cannabinoid receptor (CB1) mediates inhibition of nitric oxide production by rat microglial cells. "J Pharmacol Exp Ther". 288 (1999) 3 1357-66.
- YAZULLA, S. (2008) - Endocannabinoids in the retina: from marijuana to neuroprotection. "Prog Retin Eye Res". 27 (2008) 5 501-26.
- YAZULLA, S.; STUDHOLME, K. M.; MCINTOSH, H. H.; DEUTSCH, D. G. (1999) - Immunocytochemical localization of cannabinoid CB1 receptor and fatty acid amide hydrolase in rat retina. "J Comp Neurol". 415 (1999) 1 80-90.
- ZEISS, C. J. (2013) - Translational models of ocular disease. "Vet Ophthalmol". 16 Suppl 1 (2013) 15-33.
- ZHANG, C.; WANG, H.; NIE, J.; WANG, F. (2014) - Protective factors in diabetic retinopathy: focus on blood-retinal barrier. "Discov Med". 18 (2014) 98 105-12.
- ZHONG, L.; GENG, L.; NJIE, Y.; FENG, W.; SONG, Z. H. (2005) - CB2 cannabinoid receptors in

## References

trabecular meshwork cells mediate JWH015-induced enhancement of aqueous humor outflow facility. "Invest Ophthalmol Vis Sci". 46 (2005) 6 1988-92.